AN ESSENTIAL PHOSPHOINOSITIDE SPECIFIC PHOSPHOLIPASE C LIKE PROTEIN IN *TRYPANOSOMA BRUCEI*

by

NÚRIA WADDINGTON NEGRÃO

(Under the Direction of ROBERTO DOCAMPO)

ABSTRACT

Trypanosoma brucei is the causative agent of African Trypanosomiasis, a deadly disease affecting humans and cattle. The inositol 1,4,5 triphosphate/diacylglycerol (IP_3/DAG) pathway regulates important processes in many organisms. *T. brucei* has an active IP_3 receptor, localized to the acidocalcisome, that is essential for infection in mice. *T. brucei* has a phosphoinositide phospholipase C (*TbPI-PLC*, Tb927.11.5970) that hydrolyses phosphatidylinositol (PI) and phosphatidylinositol 4,5-bisphosphate (PIP_2). However, knockdown of *TbPI-PLC* expression by RNAi did not affect growth. Here we investigate if a PI-PLC-like protein (*TbPI-PLC-like*, Tb927.6.2090) is involved in the IP_3/DAG pathway. *TbPI-PLC-like* was identified in a proteomics study of palmitoylated proteins of *T. brucei*, and it is a highly conserved protein in all Trypanosomatids. The protein has an X catalytic domain but lacks the Y catalytic domain possessing instead a PDZ domain, in addition it has an has an *N*-terminal myristoylation consensus sequence. Recombinant *TbPI-PLC-like* does not hydrolyze PI or PIP_2 and does not bind to IP_3. Knockdown of *TbPI-PLC-like*

expression by RNAi did not change the levels of IP_6 in the cells. Taken together these results suggest that *TbPI-PLC-like* is not involved in the IP_3/DAG pathway. We also tested if *TbPI-PLC-like* was a modulator of *TbPI-PLC*. Recombinant *TbPI-PLC-like* did not modulate *TbPI-PLC* activity and knockdown of *TbPI-PLC-like* expression by RNAi did not affect the expression of *TbPI-PLC*. However, it did result in growth inhibition and decreased virulence *in vivo* indicating that this protein is important for the parasite. Preliminary mass spectrometry analysis of the possible binding partners of *TbPI-PLC-like* show strong interactions with the translational machinery.

INDEX WORDS: *Trypanosoma brucei*, Phospholipase C, PDZ, Pseudoenzyme

AN ESSENTIAL PHOSPHOINOSITIDE SPECIFIC PHOSPHOLIPASE C LIKE PROTEIN IN *TRYPANOSOMA BRUCEI*

by

NÚRIA WADDINGTON NEGRÃO

B.Sc., University of Cape Town, South Africa, 2006

B.Sc. Honors, University of Cape Town, South Africa, 2007

A Dissertation Submitted to the Graduate Faculty of The University of Georgia in Partial Fulfillment of the Requirements for the Degree

DOCTOR OF PHILOSOPHY

ATHENS, GEORGIA

2019

AN ESSENTIAL PHOSPHOINOSITIDE SPECIFIC PHOSPHOLIPASE C LIKE PROTEIN IN *TRYPANOSOMA BRUCEI*

by

NÚRIA WADDINGTON NEGRÃO

Major Professor:	Roberto Docampo
Committee:	Cordula Schulz
	Karl Lechtreck
	Kojo Mensa-Wilmot

Electronic Version Approved:

Ron Walcott
Interim Dean of the Graduate School
The University of Georgia
December 2019

DEDICATION

I dedicate this work to my family. My father José Guilherme Mingot Maurício Negrão, my mother Clotilde Isabel Silva Waddington, my stepmother Sabina Asselle, and my siblings Nayra Waddington Negrão, Kiúri Waddington Negrão, and Maia Asselle Negrão. I also dedicate it to my partner David Bridgforth.

For everything that I am, I am because of you.

ACKNOWLEDGEMENTS

I would like to extend my deepest gratitude to my major professor, Dr. Roberto Docampo, for his guidance and encouragement throughout the past five years. Dr. Docampo created the perfect environment for me to explore and grow scientifically. He balanced enough guidance so I wouldn't veer too far off track, and plenty of freedom so I could try things to my satisfaction. Because he trusted in me, I re-learned to trust in myself. That is an invaluable gift.

I would also like to thank my committee members, Dr. Cordula Schulz, Dr. Karl Lechtreck, and Dr. Kojo Mensa-Wilmot. The development of this project would not have been possible without their input and direction.

I would not be here today without the many long talks with Dr. Silvia Moreno where she encouraged me to keep at it. Dr. Moreno always had my best interests at heart and she helped me navigate difficult situations in a successful way. I learned a lot from Dr. Moreno and I am very grateful for everything she did.

A few people were instrumental for getting experiments done and moving this project along. Dr. Guozhong Huang gave me technical support on every step of the way. Dr. Sharon King-Keller for technical help and guidance for the enzyme assays. Dr. Myriam Hortua for technical guidance and support on biochemical experiments, and the mouse infections. Dr. Ciro Cordeiro for technical advice on molecular, cell culture and animal experiments. Dr. Brian Suarez for the inositol phosphate mass spectrometry experiments. Dr. Kandasamy and the Biomedical

Microscopy Core for showing me how to use the microscopes. Dr. Chou and Dr. Dennis Phillips (Proteomics and Mass Spectrometry Facility). Dr. Rodrigo Baptista for bioinformatics analysis of the proteomics data, and for the phylogeny. Dr. Vicente Martins for help with some microscopy images. Melissa Storey and Beejan Asady for generating the polyclonal antibodies and for technical support.

All the other lab members of the Docampo and the Moreno labs (past and current) contributed to the successful completion of this work. I am grateful for the great lab environment of cooperation and friendship that we have created and maintained over the years. I always had people to bounce ideas off on, and to go for suggestions. I would like to thank Dr. Srinivasan Ramakrishnan and Dr. Noelia Lander for discussing my experiments and my results with me countless times.

Finally, I would like to thank my friends in this graduate school journey. They served as a source of motivation, commiseration, and inspiration. I have counted on my friends throughout this entire journey and I have enjoyed sharing it with them very much.

TABLE OF CONTENTS

Page

LIST OF TABLES

Page

LIST OF FIGURES

Page

CHAPTER 1

INTRODUCTION AND LITERATURE REVIEW

Most of our knowledge about eukaryotic cellular biology comes from a very limited set of organisms. Almost all work has been done in a handful of immortalized mammalian cell lines, a few animal model organisms, two species of yeast, and *Arabidopsis thaliana*. Considering that animals and fungi belong to the same supergroup of Eukaryotes, the ophisthokonta, we aren't even scratching the surface of eukaryotic diversity. This is part of what makes studying protists so intriguing, we are bound to discover new aspects of cellular biology as part of our work (it can also make it challenging, as tools and paradigms that are well established elsewhere don't always work as well in these organisms).

Trypanosoma brucei

Trypanosomatids are a diverse family of flagellated protozoan parasites transmitted by various vectors like leeches, biting flies and bugs, that infect almost all vertebrate classes[1,2]. Species belonging to two genera, *Trypanosoma* and *Leishmania*, are important human pathogens causing three distinct diseases, Chagas disease, HAT (Human African Trypanosomiasis, also known as sleeping sickness) and leishmaniasis, that primarily and disproportionally affect the poorest and most isolated populations[2]. HAT is caused by two subspecies of *Trypanosoma*

brucei, *Trypanosoma brucei gambiense* (90% of cases) and *Trypanosoma brucei rhodesiense* (10% of cases). Infection with either parasite results in death if left untreated and both have similar clinical signs and symptoms[3]. The parasite is transmitted via the bite of the tsetse fly (genus: *Glossina*) and reproduces in the blood and the lymphatic system causing the first stage of the disease, with symptoms that are characteristic of a generalized infection such as intermittent fever, pain, weakness, anemia, and dermatological symptoms. After a variable period of time, that is shorter in infections with *T. b. rhodesiense*, the parasite crosses the blood-brain barrier and invades the central nervous system causing the second stage of the disease (meningo-encephalitic stage), with progressive neurological damage, sleep disturbances and neuro-psychiatric disorders[3,4]. There is no vaccine available to prevent HAT and only five chemotherapy drugs. Most of the drugs are used as a single drug regimen and have been in clinical use for more than 50 years[5]. The World Health Organization (WHO) estimates that 1,000 new cases of HAT occur each year and that there are currently 57 million people at risk of contracting it.

T. brucei can also infect domestic and wild animals, and is therefore an important veterinary disease agent[6]. Animal African Trypanosomiasis (AAT, commonly referred to as “nagana”), the disease that affects cattle, is caused by a number of trypanosomes. The most clinically important species are *T. vivax*, *T. congolense* and *T. brucei brucei*. The disease in cattle is characterized by substantial weight loss making the animals progressively weaker and unfit for work, creating an economic barrier for development and food production[6].

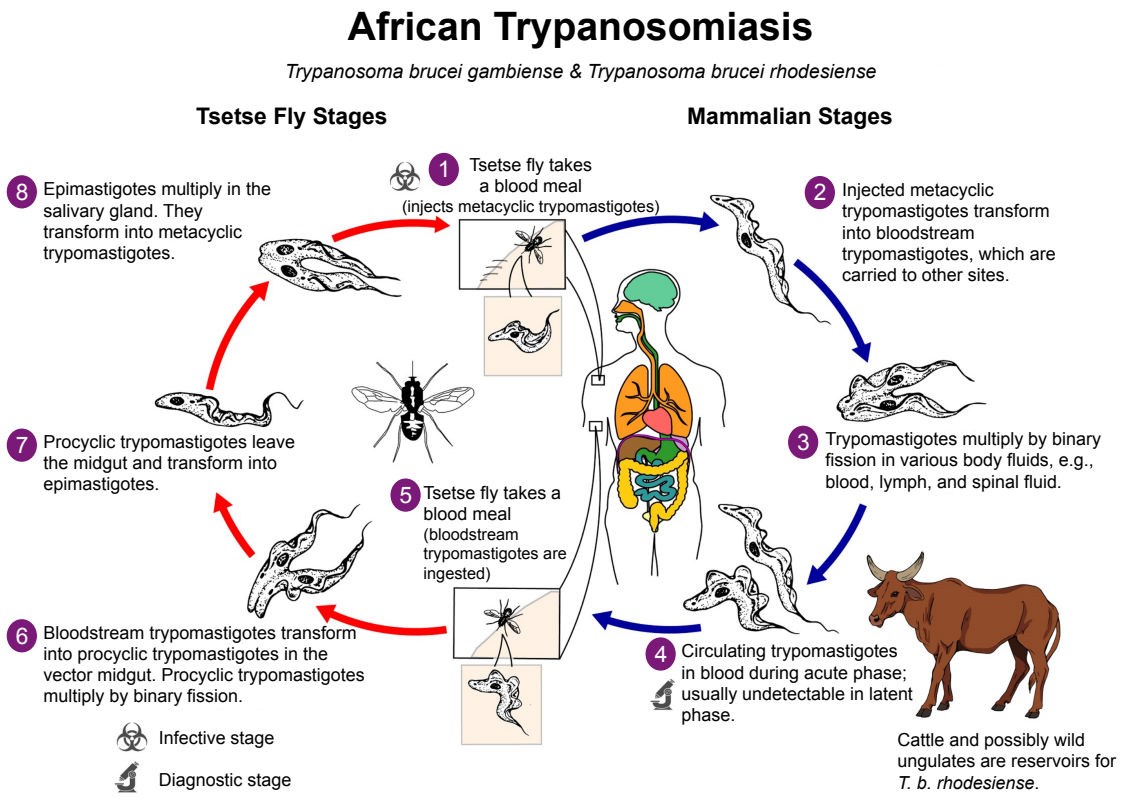

Figure 1. Life cycle of *Trypanosoma brucei*.
Infection begins when (1) a tsetse fly takes a blood meal, injecting metacyclic trypomastigotes into the mammalian host. (2) The metacyclic trypomastigotes transform into bloodstream trypomastigotes and are transported to other sites. (3) The trypomastigotes multiply by binary fission in various body fluids, like the blood, lymph and spinal fluid. (4) During the acute phase of the disease it is possible to detect circulating trypomastigotes in the blood; these are usually undetectable in the latent phase. (5) A second tsetse fly takes a blood meal, ingesting bloodstream trypomastigotes. (6) Bloodstream trypomastigotes transform into procyclic trypomastigotes in the midgut of the vector, and multiply by binary fission. (7) Procyclic trypomastigotes leave the midgut and transform into epimastigotes. (8) Epimastigotes multiply in the salivary gland and transform into trypomastigotes, ready to be injected into the next host. (Figure adapted from the CDC website).

Figure 1 shows the life cycle of *T. b. gambiense* and *T. b. rhodesiense*. The other African trypanosomes have a similar life cycle except that cattle and wild ungulates are the mammalian host. The bite of an infected tsetse fly begins the infection in the mammalian host. Injected metacyclic trypomastigotes transform into bloodstream trypomastigotes which divide in the blood, lymph and spinal fluid by binary fission. When a second fly takes a blood meal it ingests circulating bloodstream trypomastigotes which transform into procyclic trypomastigotes in the gut. The procyclic trypomastigotes transform into epimastigotes and migrate to the salivary gland of the fly where they divide and transform back into metacyclic trypomastigotes. *T. b. brucei* (*T. brucei*) does not cause disease in humans and is the organism that we used for this study. *T. brucei* is a well characterized model organism, amenable to reverse genetic approaches, and used to study general biological processes[7]. The *T. brucei* genome (about 9000 protein-coding genes) has been sequenced and annotated for the two commonly used laboratory strains, *T. brucei* 927 and *T. brucei* 427. The insect (procyclic – PCF) and the mammalian bloodstream (BSF) forms can be grown and maintained in cell culture, and in suitable animal models (tsetse flies, rodents) allowing for the study of host-pathogen interactions[8]. In vitro differentiation of BSF to PCF allows for the study of changes in gene expression and metabolism over the life-cycle of the parasite[9]. This is particularly interesting for processes involving organelles like the mitochondrion and glycosomes that have very different metabolic functions in the two life stages[10]. In this study we use the 427 strain of *T. brucei* to study a previously uncharacterized essential protein.

Phosphate and inositol

Phosphorous is one of the most important elements for life, normally found combined with oxygen in the form of phosphate (PO_3^-, also known as inorganic phosphate - Pi). Adding (phosphorylation) and removing (dephosphorylation) phosphate from proteins is the most frequent eukaryotic post-translational modification and it regulates nearly every aspect of cell life[11,12]. Nucleoside triphosphates release high amounts of energy when hydrolyzed to diphosphate or monophosphate driving virtually all biochemical reactions[13]. Due to this central role, availability of phosphate is tightly controlled and cells have developed many mechanisms to regulate its transfer and storage. One of the ways that cells store phosphate is as a linear polymer formed by phospho-anhydride bonds called polyphosphate (polyP)[14]. In yeast and in *T. brucei* inositol pyrophosphates (PP-IPs) regulate the metabolism of polyP[15]. Inositol is a metabolically inert six carbon ring that serves as the building block for two classes of small molecules, the soluble inositol phosphates (of which PP-IPs are part)[16], and the phosphorylated inositol lipids (phosphoinositides)[17].

When the inositol ring is linked to diacylglycerol via a phosphodiester link it forms phosphatidylinositol (PI), which represents about 15% of total phospholipids in the cell[18]. PI is synthesized in the endoplasmic reticulum and then transported to cellular membranes via vesicular trafficking and by several transfer proteins[17,18]. The inositol ring of PI can be reversibly phosphorylated forming seven species of phosphoinositides[18], the most abundant being phosphatidylinositol-4-phosphate (PI(4)P) and phosphatidylinositol-4,5-bisphosphate ($PI(4,5)P_2$ – PIP_2 used in this

text for simplicity). The distribution of the various species of phosphoinositides on the cell membranes is not homogeneous. For example, PIP_2 and $PI(3,4,5)P_3$ are concentrated at the plasma membrane enriched in lipid rafts, while PI(3)P is concentrated in early endosomes[18]. This means that phosphoinositides serve as a molecular marker of organelles[19,20]. In addition to their structural role as part of the lipid bilayer, phosphoinosites participate in signaling pathways via binding to cytosolic proteins or to the cytosolic domains of membrane proteins. The binding to and hydrolysis of PIP_2 by phospholipase C (PLC) resulting in the formation of inositol-1,4,5-trisphosphate (IP_3) followed by release of calcium into the cytosol is probably the best recognized signaling cascade involving phosphoinositides. This is also the most well characterized pathway for the synthesis of the soluble inositol phosphates[21].

Inositol phosphates are a family of small molecules formed by the phosphorylation and pyrophosphorylation of the inositol ring. The inositol ring can be phosphorylated in such a way to form 64 unique molecules, the majority of which have been identified in the eukaryotic cell[13]. The fully phosphorylated inositol hexakisphosphate (IP_6), also known as phytic acid, is the most abundant form[22]. Inositol pyrophosphates, the molecules that regulate the metabolism of polyP, are generated when a pyrophospho-anhydride bond is created by phosphorylation. For example, IP_6 is phosphorylated by inositol hexakisphosphate kinase (IP6K) to form 5-diphospho-inositol 1,2,4,5,6-pentakisphosphate (5PP-IP_5 or IP_7).

PLCs and IP_3 in *T. brucei*

As mentioned above, the first step in the formation of soluble inositol phosphates is the hydrolysis of PIP_2 by a phosphoinositide specific phospholipase C (PI-PLC). There are 13 mammalian PI-PLC isozymes that can be grouped into six classes based on their structure and how they are activated. The core domains, shared by all PI-PLCs, are: an EF-hand motif on the N-terminus that may play an important part in stabilizing the fold of the enzyme as well as binding to calcium[23]; a split TIM alpha/beta barrel that is composed of an X and Y domains forming the catalytic core, with the amino acids between these two domains serving an auto-inhibitory function[24]; and a C2 domain, a calcium-dependent membrane targeting domain, on the C-terminus. In addition to these core domains, most PI-PLCs also have a pleckstrin homology (PH) domain that binds to the phosphoinositide and each class has its own additional regulatory domains[24]. PI-PLCs are cytosolic proteins that need to be activated by a signal, usually a rise in cytosolic calcium, to move to the plasma membrane and hydrolyze PIP_2. This movement to the plasma membrane is regulated in a different way in each class of PI-PLCs[25].

The PI-PLCs of trypanosomatids resemble the simplest mammalian PI-PLC, PLC zeta that is produced in sperm cells, transferred to the oocyte during fertilization, and is responsible for the calcium spikes that activate the egg[25]. PLC zeta is different from other PI-PLCs in two important ways. It hydrolyzes PIP_2 present on the membrane of cytoplasmic vesicles, instead of on the plasma membrane, and it is constitutively active being regulated by degradation[25]. The PI-PLCs of *Leishmania amazonensis* (LAMA_000614900), *T. cruzi*

(TcCLB.504149.160) and *T. brucei* (Tb927.11.5970) all have a similar domain organization to PLC zeta, possessing all the canonical PI-PLC domains described above (EF-hand, X, Y and C2). In addition, the *T. cruzi* and *T. brucei* PI-PLCs have a myristoylation consensus sequence on the N-terminus, while *L. amazonensis* does not. Metabolic labeling with ^{3}H-myristate and ^{3}H-palmitate demonstrated that *TcPI-PLC* is lipid modified *in vivo*[26]. The lipid modifications of the *T. cruzi* PI-PLC, myristoylation of a glycine residue in the second position and acetylation of a cysteine in the fourth position, are sufficient and necessary to target the protein to the outer surface of the plasma membrane[27]. The protein has two peaks of expression during the developmental cycle of *T. cruzi*, first when the parasite transforms from trypomastigotes to amastigotes and then again when the parasite goes from amastigotes to trypomastigotes[28]. *TcPI-PLC* stimulates the hydrolysis of host PIP_2, a novel mechanism of host-pathogen interaction[28]. The *T. brucei* PI-PLC (*TbPI-PLC*) has a punctate distribution in the cytoplasm and the plasma membrane of the parasite. The myristoylation consensus sequence at the N-terminus is sufficient and necessary for the localization of *TbPI-PLC* at the plasma membrane. Knockdown of *TbPI-PLC* by RNA interference did not affect growth in cell culture, however it also did not completely abolish PI-PLC activity in cell lysates suggesting that the knockdown was incomplete and some protein was still present[29]. The recombinant protein had maximum activity at cytosolic calcium levels, making it constitutively active, with a lower reaction rate (V_{max}) than other PI-PLCs[29].

Cytosolic IP_3 is generated as a result of PI-PLC activity. IP_3 acts as a messenger that binds to an IP_3 receptor (IP_3R) resulting in calcium release to the cytosol. Calcium signaling is important for many biological processes[30-32]. Trypanosomatids have many signaling and regulatory proteins that bind calcium, and calcium signaling is important for host cell invasion of intracellular trypanosomatids[33-35]. The IP_3R of *T. brucei* is an essential protein localized to the acidocalcisomes, releasing calcium from these organelles instead of the endoplasmic reticulum[36]. Acidocalcisomes are lysosome-related organelles, first described in trypanosomatids[37,38], and are the main calcium store in trypanosomes[39]. They are in close contact with the mitochondrion, which has an essential mitochondrial calcium uniporter[40], allowing for rapid calcium transfer across the membranes of the two organelles[41]. In order to control its effects, cytosolic IP_3 is rapidly phosphorylated, by inositol polyphosphate multikinase (IPMK), to successively form $I(1,3,4,5)P_4$ and $I(1,3,4,5,6)P_5$[15]. The *T. brucei* IPMK is also an essential enzyme[42], underlining the importance of the inositol phosphate pathway in this organism.

In addition to the PI-PLC *T. brucei* also has a GPI-PLC[43-45]. GPI (glycoylphosphatidylinositol) is a lipid anchor for many cell-surface proteins[46]. The GPI anchor is assembled in the endoplasmic reticulum, and it consists of a phosphatidylinositol, glycans comprising one glucoseamine and three mannoses, and a terminal phosphoethanolamine, which is amide-bonded to the newly formed carboxyl terminus of a protein during the process of GPI attachment[46,47]. The lipid can be a 1-alkyl-2-acyl phosphatidylinositol, diacyl phosphatidylinositol, or inositol-

phosphoceramide. In some cases, the inositol ring is palmitoylated or myristoylated[46,48]. The carboxyl terminus of GPI-anchored proteins has a hydrophobic signal sequence that is clipped off and replaced via a transamidation reaction with a preassembled GPI anchor. The GPI is further modified in the endoplasmic reticulum and the Golgi, and then the proteins are transported to the cell surface[48]. The *T. brucei* GPI-PLC (*TbGPI-PLC*) contributes to the cleavage of the GPI anchor of the variant surface glycoprotein (VSG), and release of the surface coat during differentiation. BSF trypanosomes are covered by VSG, a predominant surface antigen, and variation in the expression of these proteins (VSGs) allows the parasites to persist and escape the immune system of the hosts[49,50]. The VSG coat is essential for survival *in vitro* and *in vivo*[51], and it functions as part of the survival strategy of individual cells through rapid endocytosis, removal of bound antibody and recycling back to the cell surface[52-54].

PLC-like proteins

In addition to the 13 PI-PLC isozymes mentioned above, mammalian cells also have a related family of pseudoenzymes designated PLC-related but catalytically inactive protein (PRIP) family[58]. The PRIP pseudoenzymes have the same domain organization as the PLC delta isozymes. However, they are larger proteins with unique regions at the N and C-terminus and more importantly, the residues within the catalytic domains critical for PLC activity are not conserved[59] and therefore they are not active[59-61]. PRIP pseudoenzymes act as scaffolding proteins that bind and recruit phosphatases (PP1 and PP2A) to required sites in

the cell. When the target proteins (of the phosphatases) get phosphorylated, PRIP also gets phosphorylated and releases the phosphatases which stop the signaling[58].

The PRIP family is an example of a pseudoenzyme family. Recently pseudoenzymes have been defined as “the predicted catalytically defective counterparts of enzymes owing to an absence of one or more catalytic residue.”[62] Pseudoenzymes are thought to arise after gene duplication events, and they share a similar overall protein fold when compared with their catalytically active counterparts[63,64]. The functions of pseudoenzymes can be grouped into four paradigms: (i) allosteric regulation of conventional enzymes, (ii) integrators of signaling events and/or acting as molecular switches, (iii) controlling assembly and localization of signaling hubs, or (iv) competing for binding of substrates/subunits to control the activity of conventional enzymes[65]. Historically, the study of pseudoenzymes has been bypassed in favor of their active counterparts. However, the ubiquitous presence of pseudoenzyme families in every organism and the sequence conservation of these expressed proteins emphasizes their possible biological importance. In this study we will be investigating the function of a predicted pseudoenzyme related to the *T. brucei* PI-PLC.

CHAPTER 2

AN ESSENTIAL PHOSPHOINOSITIDE SPECIFIC PHOSPHOLIPASE C LIKE PROTEIN IN *TRYPANOSOMA BRUCEI*

Introduction

Soluble inositol phosphates (IPs) and the lipid-bound inositols, phosphoinositides (PIs), are highly regulated small molecules important for various cell functions[13,21,22]. A non-exhaustive list include phosphate homeostasis[66-68], DNA repair by homologous recombination[69,70], membrane trafficking[71], cytokinesis[72], maintenance of telomere length[73,74], apoptosis[75,76], transcription of glycolytic enzymes[77], insulin secretion[78], epigenetic modifications to chromatin[79], cytoskeletal reorganization[80,81], and autophagy[82]. In *Trypanosoma brucei*, IPs regulate polyphosphate synthesis[15], phosphate release from the acidocalcisome[83], life stage development[84], and calcium (Ca^{2+}) signaling[29].

The *myo*-inositol ring is the precursor to all inositol molecules[21]. *Myo*-inositol can be attached to a lipid (usually diacylglycerol – DAG) through a diester phosphate to the 1-hydroxyl of the ring to form phosphatidylinositol (PI). PI can be further phosphorylated on the inositol ring giving rise to the other phosphoinositides. When it remains in the cytosol the *myo*-inositol ring serves as a building block that can be phosphorylated at various positions forming the inositol phosphates, of which the fully phosphorylated inositol hexakisphosphate (IP_6, also

known as phytic acid) is the most abundant in the cell[22]. Figure 2 shows a simplified pathway for the synthesis of inositol phosphates in *T. brucei*. The most well studied route begins with the formation of inositol 1,4,5-triphosphate (IP_3) as a result of the cleavage of phosphatidylinositol 4,5-bisphosphate (PIP_2) by a phosphoinositide-specific phospholipase C (PI-PLC)[29]. Free cytosolic IP_3 can be dephosphorylated to form *myo*-inositol, or it can be phosphorylated all the way to bisdiphosphoinositol tetrakisphosphate (IP_8) (Figure 2). We have previously characterized the activity of the inositol phosphate multikinase (IPMK), the inositol pentakisphosphate kinase (IP5K), and the inositol hexakisphosphate kinase (IP6K) from *T. brucei*[15]. The model organism *Dictyostelium discoideum* has a cytosolic route for the formation of inositol phosphates via direct phosphorylation of *myo*-inositol[85,86]. There is also evidence that a cytosolic route exists in plants[87]. Although we do not have direct evidence of this cytosolic route in *T. brucei*, we cannot rule out a similar pathway in the parasite.

T. brucei has an essential IP_3 receptor (IP_3R) in the acidocalcisome that releases calcium when bound to IP_3[36], and the IPMK which phosphorylates IP_3 is also essential[42]. However, knockdown of the expression of the *T. brucei* PI-PLC by RNA interference did not result in a delay in growth, indicating that it is not essential[29]. In addition, the *TbPI-PLC* is activated at cytosolic calcium levels and its maximum velocity (V_{max} – the rate an enzyme catalyzes a reaction) is thirty times lower than V_{max} of the *Trypanosoma cruzi* PI-PLC[29]. These results were surprising because typically PI-PLCs hydrolyze PIP_2 rapidly in response to a signal. This seems to indicate that *T. brucei* might regulate the formation or

availability of IP_3 in a different way from other organisms. In this study we investigate if a protein that was annotated as a PI-PLC-like is involved in the inositol pathway in *T. brucei*.

Experimental Procedures

Chemicals and Reagents

Mouse antibodies against HA were from Covance (Hollywood, FL). Mouse antibodies against c-Myc, Hemin, P8340 protease inhibitor, TRI reagent, and other analytical reagents were from Sigma-Aldrich (St. Louis, MO). Goat secondary antibodies were from LI-COR Biosciences (Lincoln, NE). Phusion HF DNA polymerase, P8340 protease inhibitor, protease inhibitors, HisPur™ Ni-NTA Chromatography Cartridge was from Thermo Fisher Scientific (USA). Laemmli sample buffer was from Bio-Rad Laboratories (Hercules, CA). Acrylamide mix was from National Diagnostics (Chapel Hill, NC). The bicinchoninic (BCA) protein assay kit and the Silver Stain kit were from Pierce (Thermo Fisher Scientific, USA). BenchMark Protein Ladder, Alexa-conjugated secondary antibodies, Hygromycin B, and *Escherichia coli* BL21 Codon Plus (DE3)-RIPL were purchased from Invitrogen (Carlsbad, CA). Benzonase® Nuclease, anti-Histidine tag antibodies, vector pQE-80L were from Novagen (EDM Millipore, Billerica, MA). ^{3}H-PIP_2 (15-30 Ci/mmol) and ^{3}H-IP_3 (15-30 Ci/mmol) were from Perkin Elmer (Waltham, MA). Fetal Bovine Serum was from Atlanta Biologicals (Atlanta, GA). G418 disulfate was from Teknova (Hollister, CA). T4 DNA Ligase from Promega (Madison, WI). The

p2T7^{Ti}B/GFP vector was a gift from Dr. John Donelson (University of Iowa, Iowa City, IA). Primers were ordered from IDT (Coralville, IO).

Bioinformatic analysis

General information available for *TbPI-PLC-like* (Tb927.6.2090; NCBI: XP_845330.1) and *TbPI-PLC* (Tb927.11.5970; NCBI: XP_828672.1) was obtained from TriTrypDB[88] (TriTrypDB.org). For the following analysis the entire amino acid sequences deduced from the nucleotide sequences of the ORFs were used as the query. Myristoylation prediction was done using NMT – The MYR Predictor[89] (http://mendel.imp.ac.at/myristate/SUPLpredictor.htm), and the Myristoylator[90] (web.expasy.org/myristoylator/). Functional analysis, classification into families and prediction of domains was done using InterPro[91] (ebi.ac.uk/interpro/). We used Clustal Omega[92] (ebi.ac.uk/Tools/msa/clustalo/) for DNA and protein sequence alignments and to calculate identity between sequences. The I-TASSER server[93-95] was used to generate a structural model and predict binding partners for *TbPI-PLC-like*. Orthology analysis was done using OrthoMCL DB[96] (orthomcl.org).

For the phylogenetic analysis we selected all the orthologs identified by TriTrypDB and generated an alignment using MAFFT[97]. The archive with the aligned proteins was submitted to Modeltest[98] for prediction of the best model for amino acid substitution, which was Jones-Taylor-Thornton (JTT) with Gamma distribution (+G). This model was used to generate the maximum likelihood tree using PhyML[99] with 1,000 bootstrap replicates. Bootstrap values below 70% were removed for clarity, being that these don't have statistical support.

Cloning, heterologous expression and purification of recombinant *Tb*PI-PLC-like

The DNA sequence of *TbPI-PLC-like* was PCR-amplified from *T. brucei* Lister strain 427 genomic DNA with specific primers carrying *BamHI* and *HindIII* restriction enzyme sites (Table 1). The purified PCR product and the prokaryotic expression vector pQE-80L (His-tag at the N-terminus) were digested overnight with the restriction enzymes *BamHI* and *HindIII*. The digested DNA fragments were gel purified, ligated using T4 DNA Ligase, and transformed into *Escherichia coli* DH5α. The sequence of several recombinant clones was verified and they were transformed into *E. coli* BL21 Codon Plus (DE3)-RIPL chemically competent cells. Protein expression was induced with 0.5 mM isopropyl β-D-1-thiogalactopyranoside (IPTG) in Luria Bertani broth overnight at 25°C. The protein was purified using affinity chromatography HisPur^{TM} Ni-NTA Chromatography Cartridge, according to the manufacturer's instructions, and identified by SDS-PAGE and western blot. The purified recombinant protein was used as an antigen to make polyclonal antibodies in mice. Final bleeds from six inoculated mice were affinity purified by immunoadsorption to the recombinant protein immobilized on nitrocellulose strips. The adsorbed antibodies were eluted with 0.1 M glycine, pH 2.5, and neutral pH was restored immediately by adding 1 M Tris-HCL buffer, pH 8.0.

Enzymatic assays

PI-PLC activity assay

The protein concentration was determined by BCA assay, and the recombinant protein was stored in 40% glycerol at -80°C. The PI-PLC enzymatic activity assay was performed as described previously[26] by measuring the release of soluble IP_3 from the hydrolysis of ^3H-PIP_2. Briefly, a 3:10 mixture of radioactive and cold PIP_2 was dried under a nitrogen stream and resuspended in a reaction buffer (50 mM HEPES-NaCl, pH 7.4, 2.5 mM EGTA, 3 mM MgCl2, 0.2 mM DTT, 0.1% Na-deoxycholate) by sonication. Recombinant *TbPI-PLC-like* (20 μg) and 10 nM of Ca^{2+} were added to the reaction, and this mixture was incubated at 37°C for 20 minutes. The reaction was stopped by the addition of chloroform-methanol-HCl (100:100:0.6) and 5 mM EGTA in 1 N HCl. Samples were centrifuged to separate the organic and aqueous phases. The aqueous phase was removed and counted using a scintillation counter.

^3H-IP_3 binding assay

Equilibrium-competition binding assay was performed as described previously[100]. Reactions were carried out for 10 minutes at 4°C in cytosol-like medium (CLM: 140 mM KCl, 20 mM NaCl, 2 mM MgCl2, 1 mM EGTA, and 20 mM PIPES, pH 7.0) containing radioactive IP_3 (0.75 nM) and recombinant *TbPI-PLC-like* (2 μg). In some experiments 10 μM of cold IP_3 was added. The reactions were stopped with ice-cold CLM containing 30% poly(ethylene glycol) 8000 and γ-globulin (600 μg) followed by centrifugation (20,000 x *g*, 20 minutes, 4°C). The

pellets were then solubilized in CLM containing 2% Triton X-100 and the radioactivity was determined using a scintillation counter.

Cell cultures

Cultivation of procyclic form (PCF) and bloodstream form (BSF) of *T. brucei* was carried out as described previously[101]. PCF Lister strain 427 were cultured at 27°C in SMD-79 medium[102] supplemented with 10% heat-inactivated fetal bovine serum (FBS) and 7.5 μg/ml of Hemin. PCF strain 29-13 (*T7RNA NEO TETR HYG*) co-expressing T7 RNA polymerase and *Tet* repressor[103] were a gift from Dr. George A. M. Cross (Rockefeller University, New York) and were cultured in the same conditions with 10% heat-inactivated Tet-tested FBS, G418 (15 μg/ml) and Hygromycin (50 μg/ml) added to the culture medium to maintain the integrated genes for T7 RNA polymerase and tetracycline repressor, respectively. BSF Lister strain 427 were cultured at 37°C, 5% CO_2, in HMI-9 medium[104] supplemented with 10% heat-inactivated FBS. BSF single marker (BSF-SM) (*T7RNAP TETR NEO*) trypanosomes[103] were a gift from Dr. G. A. M. Cross and were grown in the same conditions with 10% heat-inactivated Tet-tested FBS and G418 (2.5 μg/ml) added to the culture medium.

Construct design

Constructs of *TbPI-PLC-like* and *TbPI-PLC* were subcloned from *T. brucei* Lister strain 427 genomic DNA using specific primers (Table 1) The *TbPI-PLC-like* RNAi construct was amplified using primers designed with the RNA-iT server[105],

cloned into the tetracycline-inducible RNAi vector p2T7^{Ti}B/GFP with dual-inducible T7 promoters (phleomycin resistance)[106], and clones were verified by sequencing (Genewiz, South Plainfield, NJ). The one-step epitope tagging protocol reported previously[107] to generate cell lines with endogenous C-terminal tags was followed. We amplified by PCR a cassette from pMOTag4H (3x HA tag; hygromycin resistance) or pMOTag23M (3x c-Myc tag; puromycin resistance) using primers that contained 80 nt homologous region of the 3' end of CDS and 3'UTR of *TbPI-PLC-like* and *TbPI-PLC*. The constructs were verified by agarose gel electroporation and the PCR product was precipitated and resuspended to a concentration of 1000 ng/μl before transfection into *T. brucei* cells.

Cell transfections

T. brucei PCF trypanosomes in mid-log phase (~5 × 10^6 cells/ml) were harvested by centrifugation (1,000 x *g*, 7 minutes) and washed with ice-cold Cytomix (2 mM EGTA, 3 mM $MgCl_2$, 120 mM KCl, 0.5% glucose, 0.15 mM $CaCl_2$, 0.1 mg/ml BSA, 10 mM K_2HPO_4/KH_2PO_4, 1 mM hypoxanthine, 25 mM Hepes, pH 7.6) and resuspended in the same buffer at a density of 2.5 × 10^7 cells/ml. The cells were then mixed with 10 μg of *NotI*-linearized plasmid DNA or purified PCR products in 4 mm electroporation cuvettes and subjected to two pulses from a Bio-Rad Gene Pulser electroporator set at 1500 V, 25 μF, resting on ice 1 minute in between pulses. Stable cell lines were established under drug selection with addition of phleomycin (RNAi line, 2.5 μg/ml), hygromycin (HA tag line, 50 μg/ml) or puromycin (c-Myc tag line, 1 μg/ml).

For the BSF trypanosomes, 10 μg of DNA was used per 4 x 10^7 mid-log phase cells in 100 μl AMAXA Human T-cell Nucleofector solution. Cells were electroporated in 2 mm gap cuvettes with the program X-001 of the AMAXA Nucleofector. Following each transfection, stable transformants were selected and cloned by limiting dilution in HMI-9 medium with appropriate antibiotics (phleomycin 2.5 μg/ml, hygromycin 5μg/ml, puromycin 0.1 μg/ml) in 24-well plates.

Inositol phosphate extraction and analysis by LC-MS

The *TbPI-PLC-like* RNAi cell lines were grown with or without 1 μg/ml tetracycline. Cell densities were determined prior to extraction and then used for data normalization. The methods for inositol phosphate extraction and analysis by LC-MS were adapted from a previously published protocol[108]. After harvesting the cells, pellets were stored at -80ºC and thawed for extraction by adding 0.5 ml of 10% (w/v) freshly-prepared trichloroacetic acid (TCA) and mixing by vigorous vortexing. One volume of MS-grade ultrapure water (UP-water) was added to the samples, which were supplemented with 10 nmol of 3-deoxy-3-fluoro-D-*myo*-inositol 1,4,5-triphosphate, hexasodium salt (3F-IP_3) (EMD Millipore), used as an internal standard. Samples were vortexed and centrifuged at 12,000 x *g* for 20 min at 4ºC. Supernatants were neutralized with 3% ammonium hydroxide (v/v) and extracted with 2 ml of water-saturated diethyl ether (Sigma), vortexed and centrifuged at 2,000 x *g* for 10 min at 4ºC. The organic phase was discarded and extraction was repeated one more time. The bottom aqueous phase was then loaded into a Strata™-X-AW 33μm polymeric weak anion column (Phenomenex®)

preequilibrated with UP-water and methanol (MeOH, Merck) (1 ml each step). The column was washed with 25% MeOH and 100 mM ammonium acetate pH 7.2, and inositol phosphates were eluted by adding 1 ml of 100 mM ammonium carbonate pH 8 (Sigma), and equilibrated with 0.5 mL of 5% ultrapure acetic acid. Samples were dried under speed vacuum, resuspended in 60 µl of UP-water and filtered by passing through nanoFilter™ 0.2 µm PVDF (Thomson) prior to LC-MS analysis. Ten µl of each sample were injected onto an Agilent 1100 HPLC system equipped with a BioBasic AX anion-exchange column (150 mm, ID 2.1 mm x 150 mm, 5 µm particle size) (Thermo) to separate IPs. Analytes were detected in a Quadrupole Time-of-Flight (ToF) mass spectrometer (Micromass). IPs were eluted by running a 45-min gradient of two mobile phases: buffer system A (25% MeOH: water) and system B (300 mM ammonium carbonate, pH: 9.0). The ESI source was set in negative-ion mode, with a spray voltage of 3,000 V, ion-transfer capillary Tº at 300ºC.

Western blot analyses

Parental and mutant cell lines were harvested separately, washed twice in phosphate-buffered saline (PBS) and resuspended in RIPA buffer (150 mM NaCl, 20 mM Tris-HCl, pH 7.5, 1 mM EDTA, 1% SDS and 0.1% Triton X-100) containing a protease inhibitor cocktail (Sigma P8340) diluted 1:250, 1 mM EDTA, 1 mM phenylmethanesulfonyl fluoride (PMSF) and Benzonase® Nuclease (25 U/ml culture). The cells were incubated on ice for one hour and passed through an insulin syringe. The protein concentration of the lysate was determined using a

BCA protein assay kit. The total cell lysate was mixed with 2X Laemmli sample buffer at a 1:1 ratio (vol/vol) and incubated at 65°C for 10 minutes. The lysates were then loaded in a 10% SDS-PAGE. Separated proteins were transferred onto nitrocellulose membranes using a Bio-Rad transblot apparatus. Membranes were blocked with 5% (wt/vol) nonfat dried skim milk in PBS containing 0.5% Tween-20 (PBS-T) at 4°C overnight. The blots were incubated for one hour at room temperature with different primary antibodies: mouse antibodies against HA (1:1,000), mouse antibodies against c-Myc (1:1,000), polyclonal antibodies against *TbPI-PLC-like* (1:500), rabbit antibodies against VSG221 (1:4,000), mouse antibodies against β-Tubulin (1:40,000). After five washes with PBS-T the blots were incubated the appropriate goat secondary antibody at a dilution of 1:15,000 and developed using an Odyssey CLx Infrared Imaging System (LI-COR) according to the manufacturer instructions. Quantification of the intensity of the bands was done using ImageJ as described previously[109].

RNA Interference

Knockdown of *TbPI-PLC-like* and *TbPI-PLC* was induced with tetracycline in PCF and BSF cell lines carrying the RNAi cassette from p2T7^{Ti}B/GFP. Transcription of the dsRNA construct was induced by addition of 1 μg/ml tetracycline to cultures at a density of 2 x 10^6 cells/ml (PCF) or 2 x 10^5 cells/ml (BSF). Control cultures were always grown alongside for comparison. Every two days, cell cultures were passed to fresh media to the starting density. Experiments were independently replicated on at least three different occasions. Knockdown

was confirmed by qRT-PCR. RNA was isolated from control and induced cultures (10^7 cells per isolation) using TRI reagent, treated with DNase, and used as a template for cDNA synthesis with SuperScript III RNA Polymerase and oligo-dT as recommended by the manufacturer. qRT-PCR analysis was performed using specific primers (Table 1) and SYBR Green Supermix. We calculated the relative expression of *TbPI-PLC-like* and *TbPI-PLC* compared to actin using the CFX Manager™ Software (Bio-Rad).

Immunofluorescence assay

T. brucei BSF and PCF were washed with BAG and fixed with 2% paraformaldehyde in BAG for 1 hour at room temperature. Then they were adhered to poly-L-lysine coated coverslips and permeabilized with 0.1% Triton X-100 in PBS (pH 7.4) for 5 minutes. Blocking was performed overnight at 4°C in PBS (pH 8.0) containing 100 mM NH4Cl, 3% BSA, 1% fish gelatin and 5% goat serum. Cells were washed in 1% BSA in PBS (pH 8.0) and then incubated for one hour at room temperature with primary antibody: mouse polyclonal anti-*TbPI-PLC-like* (1:25), rabbit anti-*VSG221* (1:1,000), rabbit anti-*TcH$^+$ATPase* (1:50), rabbit anti-HA (1:100), mouse anti-c-Myc (1:100). Excess primary antibody was removed with a series of washes and cells were incubated with the appropriate Alexa conjugated secondary antibody (1:1,000) for one hour at room temperature. The cells were then washed and mounted to slides. DAPI (5 μg/ml) was included with the mounting medium to stain DNA. Secondary antibody controls were performed as above but in the absence of primary antibody. Differential interference contrast

(DIC) and fluorescence optical images were captured with a 100X oil immersion objective under non saturating conditions using an Olympus IX-71 inverted fluorescence microscope with a Photometrix CoolSnapHQ charge-coupled device (CCD) camera driven by DeltaVision software (Applied Precision).

Immunoprecipitation studies

TbPI-PLC-like and *TbPI-PLC* were immunoprecipitated from the single or double tagged cell lines (*TbPI-PLC*: single HA, double HA and c-Myc; *TbPI-PLC-like*: single HA, single c-Myc, double HA and c-Myc) using the Pierce HA Tag IP/Co-IP Kit according to the manufacturer's instructions. We used magnetic beads with antibodies against HA or c-Myc as well as agarose beads. Cell pellets from approximately 10^{10} cells were washed twice with warm PBS with 6 mM glucose and lysed for one hour on ice with 1% Triton X-100 in 18 ml IPP150 (10 mM Tris-HCl, pH 8.0, 150 mM NaCl, 0.1% NP40) with two dissolved tablets of Complete, EDTA-free protease inhibitor cocktail (Roche). The lysate was cleared of debris by centrifugation at 15,000 x *g* for 20 minutes at 4°C. The cleared lysate was incubated with the beads at 4°C overnight with rotation. Next the unbound lysate was collected and the beads were washed three times with TBS plus 0.05% Tween-20. Bound sample was collected with Elution Buffer and neutralized with 1M Tris, pH 9.5 (vol/vol - 1:20). Finally, samples were mixed with loading buffer, incubated at 65°C for 15 minutes and stored at -80°C. The cleared lysate, flow through (unbound lysate), and eluted sample were analyzed by 10% SDS-PAGE, Pierce Silver Stain Kit, and western blots.

For liquid chromatography tandem mass spectrometry analysis (LC-MS/MS) we compared three independent experiments. One using HA tagged *TbPI-PLC-like* cell line, one c-Myc tagged *TbPI-PLC-like* cell line, and one wild type cell line (negative control). Samples were immunoprecipitated as described above (wild type cells were incubated with anti HA magnetic beads) and then ran on a pre-cast 10% SDS-PAGE (Bio-Rad) for five minutes. The gel was then washed three times with ultrapure water, stained with SimplyBlue™ SafeStain (Invitrogen) for one hour, and de-stained with water for one hour. The bands were cut, stored in water and sent for LC-MS/MS at the Proteomics and Mass Spectrometry (PAMS) Core Facility at the University of Georgia using the Orbitrap Elite system. Results were analyzed using the Thermo Scientific Protein Discover 1.4 software and the PAMS in-house MASCOT search engine against the TriTrypDB database. For comparison between the independent experiments we normalized the intensity of each peak by dividing it by the total intensity of the run.

Yeast Two Hybrid Assay

The Matchmaker® Gold Yeast Two-Hybrid System (Takara Bio) was used according to manufacturer's instructions. We used the *Saccharomyces cerevisiae* AH109 strain and standard microbial techniques and media. YPDA is 1% (wt/vol) yeast extract, 2% (wt/vol) peptone, 2% (wt/vol) dextrose plus 100 μM adenine medium. SD medium is synthetic defined dropout medium consisting of 0.67% (wt/vol) Difco yeast nitrogen base without amino acids, 2% (wt/vol) dextrose, 2% (wt/vol) agar, 0.7% sodium phosphate dibasic, 0.3% sodium phosphate

monobasic, Sunrise amino acid / nucleotide dropout mix (e.g., a complete supplement medium CSM-Leu-Trp-His-Ade dropout complete supplement mixture lacking leucine, tryptophan, histidine, and adenine), supplemented with or without 2 mM 3-amino-1,2,4-trizole (3-AT), a histidine analog and competitive inhibitor of the *His3* gene product. The full-length c-DNAs of the *TbPI-PLC-like* and *TbPI-PLC* genes without the 5' nucleotide sequences encoding the myristoylation consensus sequence were amplified from *T. brucei* genomic DNA by PCR using specific forward and reverse primers (Table 1) containing *EcoRI* and *BamHI* restriction sites, respectively. The PCR constructs and the YTH assay bait (pGBKT7) and prey (pGADT7) expression vectors were digested with *EcoRI* and *BamHI* overnight at 37°C. Cloning was done using the Gibson Assembly Kit according to manufacturer's protocol and positive clones were confirmed by sequencing. The recombinant YTH bait and prey plasmids were cotransformed into the yeast AH109 strain by lithium acetate (LiOAc)-mediated transformation as described previously[110] and cultured successively on the dual, triple, and quadruple SD medium (SD-2DO medium minus Leu and Trp; SD-3DO medium minus Leu, Trp, and His; SD-4DO medium minus Leu, Trp, His, and Ade) for three to four days.

In vivo studies

To investigate the infectivity and virulence of *TbPI-PLC-like* p2T7 BSF trypanosomes we did an in vivo study with mice. Exponentially growing cells (*TbPI-PLC-like* p2T7 +/- tetracycline for 48 hours) were washed once in HMI-9 medium without selectable drugs and resuspended in the same medium. Eight-week-old

Balb/c mice (six per group) were infected with a single intraperitoneal injection of 2 x 10^4 BSF trypanosomes in 0.2 ml of HMI-9 medium. Mice were given either normal water or water containing 200 μg/ml doxycycline in a 5% sucrose solution[101,111]. The drinking water with or without doxycycline was provided three days before infection and replaced every two days until the end of the experiment. Animals were fed ad libitum on standard chow. Parasitemia levels were monitored everyday beginning on day three after infection[112]. Mice were euthanized when parasite density was over 1 x 10^8 cells/ml. This study was carried out in strict accordance with the recommendations in the National Institutes of Health Guide for the Care and Use of Laboratory Animals. The animal protocol was approved by the Institutional Animal Care and Use Committee (IACUC) of the University of Georgia.

Statistical analyses

All experiments were repeated at least three times with several technical replicates as indicated in the figure legends. Results were expressed as mean values ± standard deviation (SD) or standard error of the mean (SEM). Statistical analyses were performed using GraphPad Prism software Version 8.2.0. The statistical tests used are indicated in the figure legends, results are considered significant when $p < 0.05$ (individual p values are indicated in the figure legends).

Results

*Tb*PI-PLC-like sequence analysis

In their work identifying the palmitoylated proteins of *Trypanosoma brucei* Emmer et al, 2011[113] named Tb927.6.2090 (NCBI: AAZ11771) a putative phosphatidylinositol-specific phospholipase C-like (PI-PLC-like) protein. The open reading frame of *TbPI-PLC-like* is 2,699 bps and encodes a protein of 710 amino acids with a predicted molecular mass of 78.31 kDa (tritrypdb.org). *TbPI-PLC-like* has a simpler domain architecture than other PI-PLCs (Figure 3 A). Sequence similarities in amino acids 64 to 437 place the protein the PI-PLC family, and structural similarity in amino acids 263 to 594 place it in the PLC-like phosphodiesterase, TIM beta/alpha-barrel domain superfamily (InterPro). Like the previously described *T. brucei* PI-PLC (*TbPI-PLC*; Tb927.11.5970) (NCBI: XP_828672)[29] *TbPI-PLC-like* has an N-terminus myristoylation consensus sequence (amino acids 1 to 22) but it lacks an EF-hand domain. Its TIM beta/alpha-barrel is modified with an X catalytic domain (amino acids 322 to 395) and a PDZ (PSD-95-Dlg-ZO1) domain (amino acids 413 to 472) instead of a Y catalytic domain. The protein also lacks the characteristic C2 domain of PI-PLCs on the C-terminus.

The top 10 alignments from the I-TASSER analysis for *TbPI-PLC-like* were all with other PI-PLCs. The alignments had normalized Z-scores between 2.08 and 5.76 (a normalized Z-score >1 is good), and coverages varied between 0.64 and 0.92. The best alignment (0.91 coverage and normalized Z-score 5.25) was with PLC21 of *Sepia officinalis*. The top model predicted by I-TASSER had a C-score

of -0.23 (TM-score: 0.68±0.12; RMSD: 8.6±4.5Å) (Figure 3 B). C-score values range from -5 to 2, the higher the value the higher the confidence of the model, a C-score greater than -1.5 indicates a model of correct global topology. IP_3 is predicted to bind to *TbPI-PLC-like* on a loop of the PDZ domain (C-score:0.23), that is located on the inside of a pocket formed by the X domain, the PDZ domain and the rest of the TIM alpha/beta barrel sequence (Figure 3 B). The predicted model looks similar in general structure to the mammalian PLC zeta (PDB: Q86YW0) with the C-terminus, consisting of beta sheets, in between two regions with alpha helices that make up the TIM alpha/beta barrel on the one hand and the EF hand domain (PLC zeta) or PI-PLC sequence (*TbPI-PLC-like*) on the other (Figure 3 C).

TbPI-PLC-like belongs to the orthologous group OG5_151765 (orthomcl.org), a group of proteins that is specific to Kinetoplastids and highly conserved within the class (58.4% average sequence identity). TriTrypDB identified 46 potential orthologs and paralogs within EuPathDB (eupathdb.org) almost all annotated as putative or hypothetical, and all with the same domain architecture as *TbPI-PLC-like*. Sequence alignment of representative species show high conservation in the TIM alpha/beta barrel region containing the X and PDZ domains (Figure 4).

Since this gene is present in all sequenced members of Kinetoplastids but not present in any other organism it suggests that a gene duplication event occurred in the common ancestor of the class. Phylogenetic analysis (Figure 5) revealed that the PI-PLC-like of *Bodo saltans* and *Paratrypanosoma confusum* are

the most different from the other species. This was expected as *B. saltans* is a free-living kinetoplastid and *P. confusum* is an insect trypanosomatid and considered to be the link between the free-living and the obligatory parasitic species[114]. Of the trypanosomatids, the PI-PLC-like proteins of Leishmania species separated into one group together with *Endotrypanum monterogeii*, *Crithidia fasciculata*, and *Blechomonas ayalai.* All the trypanosome species are on a second group, with all *T. cruzi* strains clustering together and with a Brazilian strain of *T. rangeli*. The African trypanosomes form their own cluster.

TbPI-PLC-like does not hydrolyze PIP_2

Since *TbPI-PLC-like* has a modified TIM beta/alpha-barrel domain with a PDZ domain instead of a Y catalytic domain (Figure 3 A) we hypothesized that the protein would not hydrolyze PIP_2. In order to characterize the enzymatic activity of *Tb*PI-PLC-like we expressed it in *E. coli* as a fusion protein with an N-terminus poly-histidine tag. The recombinant protein was purified using metal-ion affinity chromatography and analyzed by SDS-PAGE and western blot (Figure 6 A-B). The recombinant protein (including the his-tag) appears as a strong band on the induced bacterial lysate (Lys) with the expected molecular mass (78.0 kDa) in the Coomassie brilliant blue staining (Figure 6 A) which is recovered as a single band after affinity purification (Purified). A band of the same size also appeared on the western blot with commercial anti-His antibodies (Figure 6 B). We tested the activity of *TbPI-PLC-like* with ^3H-PIP_2 using recombinant *TbPI-PLC* as a positive control and no enzyme as a negative control (Figure 6 C). Counts above baseline,

the no enzyme control, indicate that PIP_2 was hydrolyzed. *TbPI-PLC-like* did not hydrolyze PIP_2 *in vitro*.

TbPI-PLC-like does not bind IP_3

Cestari et al., 2018[84], used IP_3 linked to agarose beads to pull down proteins in *T. brucei* that interact with IP_3. *TbPI-PLC-like* was not pulled down with the IP_3-agarose beads[84]. However, it is notable that the IP_3-receptor was also not pulled down with the IP_3-agarose beads[84] leaving open the possibility that some IP_3 binding partners had been missed by the method. Since I-TASSER predicted that the PDZ domain of *TbPI-PLC-like* might bind to IP_3 (Figure 3 B) we decided to measure this directly using a competition binding assay with ^3H-IP_3 as described by Ding et al., 2010[100]. We recovered the recombinant *TbPI-PLC-like* after incubation with ^3H-IP_3, or a mixture of ^3H-IP_3 and cold IP_3, as can be seen on a western blot of the pelleted protein (Figure 7 A). However, we did not see a difference in radioactivity between the two conditions indicating that recombinant *TbPI-PLC-like* does not bind to IP_3 (Figure 7 B).

*Tb*PI-PLC-like does not regulate the inositol phosphate pathway

In the same study mentioned above Cestari et al., 2018[84], found that *TbPI-PLC-like* was pulled down with IP_4-agarose beads. This suggests that *TbPI-PLC-like* could be regulating the availability of IP_4. If that is the case, we would expect to see a disruption in the regulation of the inositol phosphate pathway when the expression of *TbPI-PLC-like* is reduced. Since IP_6 is the most abundant IP in the

cell, a disruption in the inositol phosphate pathway should result in a change in the total amount of IP_6. In order to investigate this, we did a knockdown of *TbPI-PLC-like* mRNA by induction of double-stranded RNAi with tetracycline and measured the amount of IP_6 in cells. Growth defects in PCF can be observed after 48 hours of RNAi (Figure 8 A). We confirmed that the expression of *TbPI-PLC-like* was knocked down by qRT-PCR (mRNA expression) and western blot (protein expression) on RNA and protein isolated from treatment and control cells (Figure 8 B-D).

We grew *T. brucei* PCF *TbPI-PLC-like* p2T7 (RNAi cell line) trypanosomes with or without tetracycline for 48 hours and measured the amount of inositol phosphates using LC-MS (Figure 9 A-B). The mass spectrometry tracings in Figure 9 A show peaks at the correct masses for IP_3, 3-flouro-IP_3 (internal standard), and IP_6. The size of the peak indicates the amount of the compound present in the sample, which is then normalized to 3-fluoro-IP_3 to allow for comparison between different runs. We found that there is no difference in the amount of IP_6 in the knockdown cells compared to control (Figure 9 B). These results indicate that *TbPI-PLC-like* is not involved in the inositol phosphate pathway.

Subcellular localization

The purified recombinant protein was used to generate polyclonal antibodies in mice. Affinity purified antibodies were tested against total cell lysates from PCF 427 WT *T. brucei* (Figure 10 A) showing a strong band at 78.0 kDa. The antibodies were used to determine the subcellular localization of *TbPI-PLC-like* in PCF and

BSF trypanosomes. In both forms *TbPI-PLC-like* has partial co-localization with membrane markers (*T. cruzi* proton ATPase in PCF, and VSG221 in BSF) (Figure 10 B). In PCF parasites the protein has a reticulated distribution in the cytosol (Figure 10 B) and it localizes to the outer surface of the plasma membrane (Figure 11).

Interaction with *TbPI-PLC*

The previously reported that *TbPI-PLC* has a high sensitivity to Ca^{2+} with maximum activity at cytosolic levels, making it constitutively active[29]. In addition, it also has a lower V_{max} than typical PI-PLCs[29], therefore producing IP_3 at a constant, low rate as opposed to rapidly and in response to a signal. This raises the question of whether *TbPI-PLC* is regulated in a different way *in vivo* from the *in vitro* regulation previously described[29], to have a higher rate of reaction in response to a stimulus like other PI-PLCs. A novel way to regulate enzyme activity has been described in *T. brucei*, where weakly active enzymes form complexes with catalytically inactive paralogs, called prozymes. The formation of these complexes increases the activity of the enzyme on average by 2000-fold[115-117]. Analysis of the alignment between the two protein sequences by Clustal Omega reveals that *TbPI-PLC-like* is 23.15% identical to *TbPI-PLC*, indicating that the two are probably paralogous. We wanted to see if *TbPI-PLC* and *TbPI-PLC-like* could form an enzyme-prozyme pair.

To investigate whether the two proteins interact with each other *in vivo* we used a previously generated cell line that has *TbPI-PLC* endogenously tagged with

hemagglutinin (HA)[29]. We tested for co-localization of the HA-tagged *TbPI-PLC* with *TbPI-PLC-like* by immunofluorescence microscopy using anti-HA antibodies and affinity-purified, polyclonal antibodies against recombinant *TbPI-PLC-like*. The two proteins have a similar sub-cellular distribution around the plasma membrane and in the cytoplasm (Figure 12 A). The overlay of the two images shows partial co-localization in vivo (Figure 12 A – Merge) with a Pearson's correlation coefficient of 0.6574. This partial co-localization in the parasite does not allow us to discard the hypothesis that the two proteins interact *in vivo*. In order to further test if there is any interaction, we used anti-HA agarose beads to immunoprecipitate *TbPI-PLC*. Western blot analysis revealed that some *TbPI-PLC-like* co-immunoprecipitates with *TbPI-PLC* (Figure 12 B). However, most of it is washed out in the flow through suggesting that the interaction might be transitory or indirect. To corroborate this weak interaction, we wanted to see whether *TbPI-PLC* would be pulled down with *TbPI-PLC-like*. We used homologous recombination to produce reciprocal double tagged cell lines where one gene was tagged with HA and the other with c-Myc (Figure 13 A). When both proteins are tagged, they do not co-localize *in vivo* and they do not co-immunoprecipitate (Figure 13 B-C). A yeast two hybrid screen yielded similar results; the two proteins had clear cytosolic expression in the yeast reporter cell line AH109, but they did not interact *in vivo* (Figure 14 A-C).

Despite the fact that we did not find evidence that the two proteins interact directly in the cell we wanted to see if their expression levels were linked to each other to rule out an indirect interaction. We tagged the *TbPI-PLC* with c-Myc in the

TbPI-PLC-like p2T7 (RNAi) cell line (Figure 15 B). Knocking down the expression of *TbPI-PLC-like* did not affect the expression of *TbPI-PLC* mRNA (Figure 15 A) or protein (Figure 15 C). Additionally, knocking down *TbPI-PLC* did not affect the protein expression of *TbPI-PLC-like* (Figure 15 D). These results lead us to conclude that these two proteins do not interact directly or indirectly in the parasite.

Growth curves and virulence

Knockdown of *TbPI-PLC-like* by use of inducible double-stranded RNA resulted in a growth defect in both PCF and BSF parasites (Figure 16 A-B). The growth defect was more pronounced in PCF cells where by day 7 of tetracycline addition the cells stopped growing and started dying. In BSF the cells grow at about half the rate than the control cells but never die off completely. Western blot analysis revealed that *TbPI-PLC-like* protein is downregulated after two days of tetracycline addition (Figure 16 A-B). To test whether this delay in growth is important for infectivity and virulence in vivo we used a mouse model. Mice infected with parasites that had *TbPI-PLC-like* knocked down survived for longer with a slightly lower parasitemia than mice infected with control parasites (Figure 17 A-B). This suggests that this protein is important for virulence during infection of a mammalian host.

Identification of proteins that bind to *TbPI-PLC-like*

In order to identify potential binding partners of *TbPI-PLC-like* we did a liquid chromatography tandem mass spectrometry analysis of proteins pulled down with

TbPI-PLC-like. We used two endogenously tagged PCF cell lines (HA and c-Myc) and wild type trypanosomes (negative control) (Figure 18 A-D). The samples were sent to the PAMS core facility at UGA. Samples were cleaved by trypsin and the resulting peptides were analyzed by LC-MS/MS. The mass spectrometry data was searched against TriTrypDB and resulted in the identification of 153 proteins in the HA cell line, 127 proteins in the c-Myc cell line, and 50 proteins in the wild type. *TbPI-PLC-like* was in the pulldown of both tagged cell lines, and was not in the wild type pulldown (Tables 2 and 3). Figure 19 shows a Venn diagram of the results from the three experiments. Of the 50 proteins from the wild type sample, 42 were shared with both the c-Myc and HA samples, six were shared with the HA sample alone, and two were exclusive to wild type. The c-Myc sample had 27 and the HA sample had 47 exclusive proteins each. The two shared 58 proteins that were not pulled down in the wild type sample. We deem these 58 proteins to be interacting specifically.

Of the 58 potential specific binding partners, one was *TbPI-PLC-like*, four were conserved hypothetical proteins, 14 were proteins that have been studied previously, and 39 have been annotated as putative proteins with a predicted function (Table 2). The list of potential *TbPI-PLC-like* binding partners is summarized in Table 2, where proteins were grouped by cellular function and sorted from highest to lowest relative abundance in the HA pull down within each group. The biggest group of identified proteins were proteins involved in translation (ribosomal proteins and translation factors, 31 proteins), some of these also had the highest abundance levels. Interestingly four RNA-binding proteins that

potentially regulate gene expression were also found. Another group of nucleotide binding proteins identified are five retrotransposon hot spot (RHS) proteins. A putative importin alpha subunit, a nuclear-pore protein that binds to the nuclear localization signal of other proteins was also identified in this study. Mitochondrial proteins, two involved in the tricarboxylic acid cycle, one mitochondrial ribosomal protein, and two other enzymes, also had high relative abundance. In addition, two glycosomal proteins were also found. This is interesting because *TbPI-PLC-like* was identified in a proteomics study of glycosomal and mitochondrial proteins[118]. Finally, three potential stress response proteins were identified, two putative heat shock 70, and one antioxidant, tryparedoxin peroxidase. The remaining putative proteins were an S-adenosylmethionine synthetase, a protein kinase with two EF-hand (Ca^{2+} binding) domains, and a cdc-2 related kinase.

We also organized the proteins based on the Mascot score. The summed scores for the individual peptides (peptide masses and peptide fragment ion masses) for all peptides that match a given protein is the Mascot score for that protein. In other words, while the intensity of the mass spectrometry peak for a given peptide is a measure of the relative abundance of that peptide in the sample (i.e. how much of the protein was there), the Mascot score is a measure of how well that peptide matches the protein sequence in the database (i.e. how good the prediction of the protein is). Table 3 summarizes the proteins identified in the LC-MS/MS analysis based on their Mascot scores. The proteins are grouped by their cellular function and sorted according to the descending Mascot score of the HA sample. The results are similar to the abundance analysis. It is noteworthy that this

approach shows that the heat shock proteins, the translation factors and the retrotransposon hot spot proteins have higher Mascot scores than the ribosomal proteins.

Discussion

Inositol phosphates play an essential role in a wide variety of cellular processes and signaling pathways in all organisms including trypanosomes[15]. However, it is not clear how the synthesis of these molecules is regulated in *T. brucei*. The only confirmed synthesis pathway is via the hydrolysis of PIP_2 by *TbPI-PLC* into IP_3, but knockdown of *TbPI-PLC* did not affect growth[29]. Since other inositol phosphates are essential to the parasite[15] the lack of a growth phenotype associated with *TbPI-PLC* raises a couple of hypotheses. *T. brucei* might have an alternative route to making soluble inositol phosphates allowing it to by-pass *TbPI-PLC*. A cytosolic route for inositol phosphate synthesis has been described in plants[87] and *D. discoideum*[85,86]. Another possibility is that activation of *TbPI-PLC in vivo* is markedly different from the reported *in vitro* activation[29], such that even very low protein levels (still present after mRNA knockdown) are sufficient to generate an adequate amount of IP_3 to sustain normal cellular function. An enzyme-prozyme pairing resulting in a reaction rate 2000-fold higher as has been described for three other *T. brucei* proteins[115-117] could generate enough IP_3.

In this study we looked at a previously uncharacterized essential protein that was classified as PI-PLC-like to see if it has a role in the inositol phosphate pathway. *TbPI-PLC-like* belongs to a highly conserved gene family in

kinetoplastids suggesting that the protein plays an important role in these organisms. Since the PI-PLC-like family is specific to kinetoplastids it is also possible that it has a novel function. The protein has general sequence and structural similarities to other PI-PLCs, but has a much simpler domain organization with a modified TIM alpha/beta barrel with a PDZ domain instead of a Y domain. PDZ are protein domains known for mediating protein-protein interactions. There are three main classes of PDZ binding domains, according to their peptide specificity, which are usually present on the C-terminus of target proteins. However, degenerate specificity and other modes of interaction have been documented. For example, some PDZ domains recognize internal peptide stretches and others form homo- and hetero-dimmers. PDZ peptide interactions have low micromolar affinities and each PDZ domain can bind to more than one PDZ binding domain[119,120]. PDZ domains are also known to bind to phosphoinosites. For example, the PDZ domains of syntenin-1 and syntenin-2 bind to PIP_2 in the plasma membrane and in the nucleus respectively[121,122]. It is estimated that between 20% and 40% of PDZ interactions are with phospholipids[121]. The PDZ domain of *TbPI-PLC-like* is homologous to those found in trypsin-like serine proteases, like DegP (HtrA), which are responsible for substrate recognition and/or binding[123]. The amino acids predicted to be involved in binding are conserved across all members of the PI-PLC-like family in kinetoplastids indicating that this could be important for the function of the protein.

We first tested whether *TbPI-PLC-like* could replace *TbPI-PLC* and synthesize IP_3 or another inositol phosphate. We showed that the PDZ domain

does not functionally replace the Y domain and *TbPI-PLC-like* does not hydrolyze PIP_2. This was expected since the Y domain of PI-PLCs is involved in the catalytic activity of the enzymes and not just in substrate binding[24]. PDZ domains are usually involved in substrate binding, and they can bind to proteins and phospholipids[121]. The I-TASSER modeling server predicted that the PDZ domain of *TbPI-PLC-like* would bind to IP_3, and the protein was pulled down with IP_4[84] which indicated that *TbPI-PLC-like* was a good candidate for a regulator of the inositol phosphate pathway. Surprisingly, *TbPI-PLC-like* did not bind to IP_3 in vitro or affect the amount of IP_6 in the cell.

We then turned to our second hypothesis, that *TbPI-PLC-like* acted as a prozyme to *TbPI-PLC* regulating its activity *in vivo*. The two proteins have a similar sub-cellular distribution; however, they don't fully co-localize. A small amount of *TbPI-PLC-like* consistently co-immunoprecipitated with *TbPI-PLC* despite most being lost in the flow through. The consistent finding in five independent experiments seems to indicate that the interaction between the two proteins is real, if weak. Tagging both proteins completely disrupted all interaction between two. It is possible that the tags themselves are interfering in the binding. The tags were added to the C-terminal end of both proteins and the C-terminal is sometimes involved in PDZ-mediated binding[119,120]. In order to more directly test whether *TbPI-PLC-like* regulates *TbPI-PLC* or vice-versa we looked at the expression of both proteins when either was knocked down. Knocking down *TbPI-PLC-like* did not affect the expression of *TbPI-PLC*, and knocking down *TbPI-PLC* did not affect the expression of *TbPI-PLC-like*. This was true at the mRNA and protein levels.

This strongly indicates that the two proteins are not important regulators of one another and dismisses the enzyme-prozyme hypothesis.

TbPI-PLC-like is expressed in both PCF and BSF, and knockdown affects the growth in both forms. This shows that the protein has a role in both life stages, though it appears to be more important for the PCFs. We also showed that *TbPI-PLC-like* is important for virulence in a mouse model of infection. The protein is expressed in the plasma membrane of both forms, and it was previously identified in a proteomics study of the flagellum of PCF parasites[124]. In PCF forms it is also prominently present in the cytosol and another study found it in a glycosomal and mitochondrial fraction of PCF parasites but not BSF[118]. In this study we report the preliminary results of a proteomic analysis of the binding partners of *TbPI-PLC-like*. The data has to be validated through the functional study of the most relevant proteins observed. We identified 57 proteins that were specifically pulled down with *TbPI-PLC-like* using two different tags (HA and Myc). We used wild type cells to eliminate proteins that bound to the beads in a non-specific manner.

None of the proteins that are involved in the inositol phosphate pathway were pulled down, including *TbPI-PLC*. This confirms the results that we reported above. There is still the possibility that un-tagged *TbPI-PLC-like* might interact with *TbPI-PLC*. One way to test that would be to do a proteomics study using the anti *TbPI-PLC-like* polyclonal antibodies for the pull down. The pull down did not identify any flagellar or membrane proteins either, which is noteworthy because *TbPI-PLC-like* was identified in a proteomics study of the flagellum of PCF trypanosomes[124].

An interesting finding was that four mitochondrial (and two glycosomal) proteins with fairly high relative abundance were identified. These results confirm a previous study that found *TbPI-PLC-like* in a cellular fraction containing these organelles[118]. Five of these proteins are involved in catabolism, from glycolysis to the TCA cycle to the electron transport chain. The sixth one is a metallo-peptidase of the M16 family that cleave the mitochondrial targeting signal as proteins are imported into the mitochondrion[125].

The largest group (35 out of 57 – 61%) of proteins identified, some with the highest relative abundance scores, in this study were ribosomal proteins, protein translation factors and RNA binding proteins. The RNA binding proteins are two DEAD-box helicases (one putative), one of which (DHH1, Tb427.10.3990) has been shown to determine the expression levels of developmentally regulated mRNAs[126]. Tb427tmp.01.5570 interacts with 5S rRNA and may be involved in ribosome biogenesis[127,128]. The fourth protein, Tb427.06.2550, has a predicted putative single-stranded RNA-binding domain[129-131] that usually binds to ribonucleoproteins or is involved in regulating RNA stability and translation[130-132]. Curiously, one of the translation factors – elongation factor Tu – is a prokaryotic protein[133] (this protein had a very low Mascot score, indicating that it could be miss-labelled). This association with protein translation, together with the association with two heat shock factors (HSP70) and one antioxidant (tryparedoxin peroxidase) raise the possibility that *TbPI-PLC-like* might act as a chaperone for protein folding.

Intriguingly, five retrotransposon hot spot (RHS) proteins with high abundance scores in the c-Myc fraction were identified (these proteins had a high Mascot score in both samples, indicating that they were correctly identified). RHSs are a multigene family that together constitute about 5% of the T. brucei genome[134]. The function of RHS proteins is not clear. However, a number of these genes are expressed in T. brucei and they appear to have a nuclear or peri-nuclear localization[134]. The RHS genes are located in subtelomeric regions of the genome and their sequences are frequently interrupted by retrotransposons that insert at the exact same relative position.

In summary, in this study we report on a PI-PLC-like protein that is essential, highly conserved and specific to kinetoplastids. We show that *TbPI-PLC-like* does not hydrolyze PIP_2 and is therefore not a PI-PLC. It also does not regulate the activity of *TbPI-PLC* or the inositol phosphate pathway. The protein has a PDZ domain and is likely to be involved in interaction with another protein or proteins. Preliminary results from a proteomics study of potential binding partners point to a possible role in protein translation.

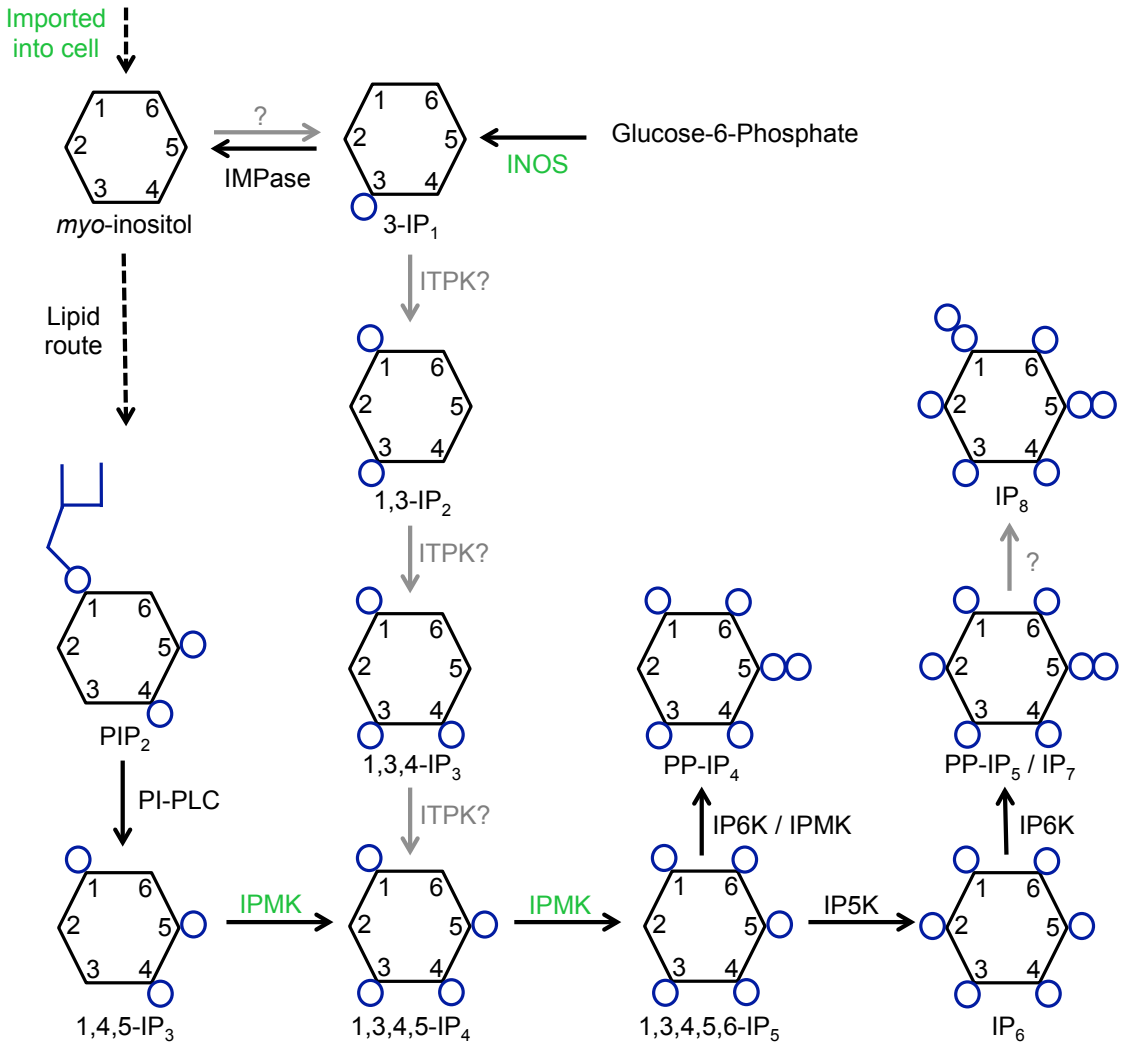

Figure 2. Pathway of inositol phosphates synthesis in *T. brucei*.
The lipid route pathway begins with the hydrolysis of PIP_2 by PI-PLC to form 1,4,5-IP_3 which is then phosphorylated to 1,3,4,5-IP_4 and 1,3,4,5,6-IP_5 by IPMK. IP5K phosphorylates 1,3,4,5,6-IP_5 to IP_6. IP6K can make PP-IP_4 and PP-IP_5. PIP_2 comes from the lipid route where *myo*-inositol is linked to diacylglycerol and phosphorylated on the membrane. *Myo*-inositol can be imported into the cell or be formed by the dephosphorylation of 3-IP_1 by IMPase. 3-IP_1 can be formed directly from glucose 6-phosphate by INOS. An alternative, fully soluble, route for the formation of IP_4 could be catalyzed by ITPK via sequential phosphorylation of 3-IP_1. Essential steps are depicted in green, unknown steps are depicted in grey.

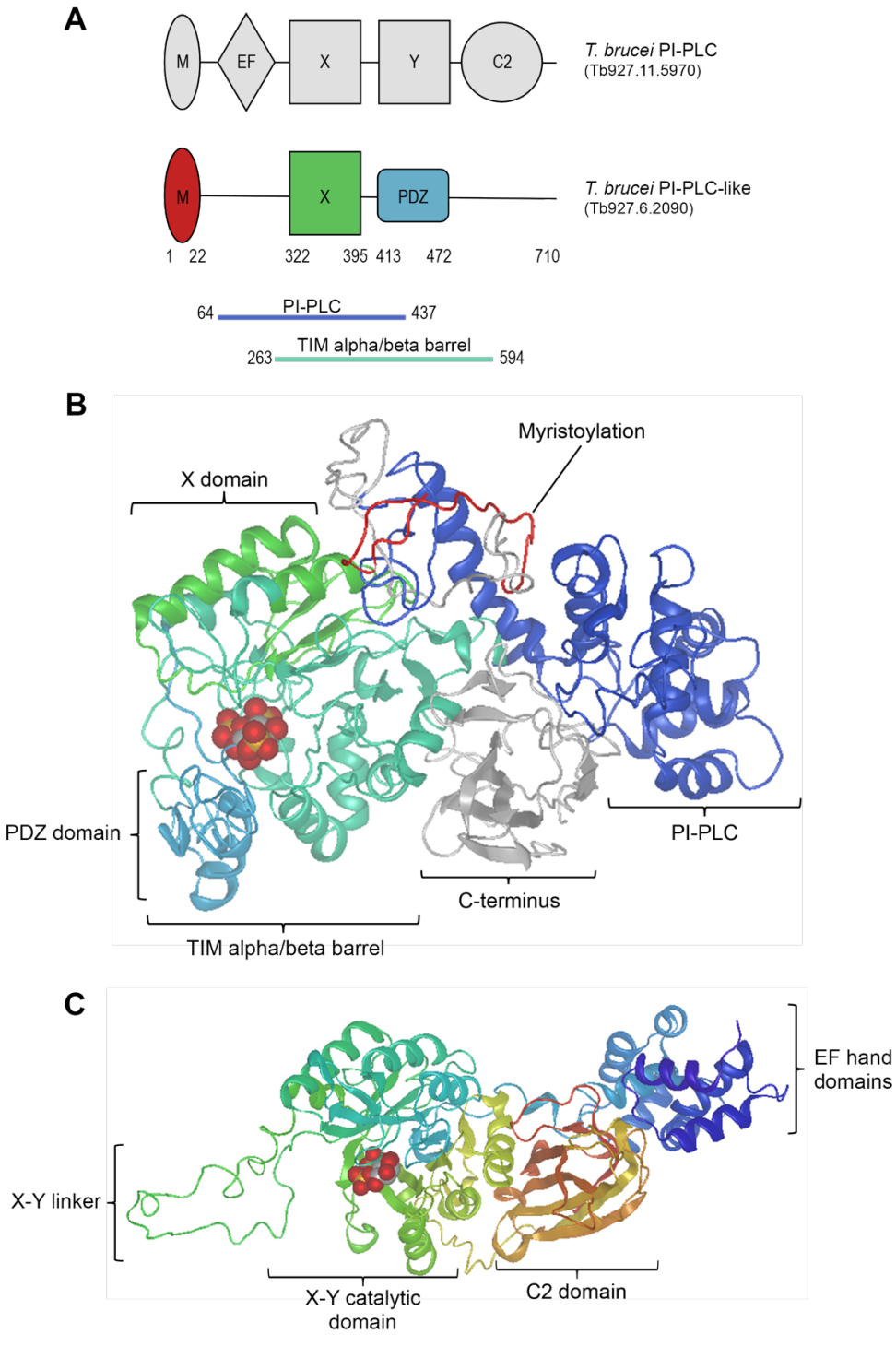
A
M
EF
X
Y
C2
T. brucei PI-PLC
(Tb927.11.5970)
M
X
PDZ
T. brucei PI-PLC-like
(Tb927.6.2090)
1
22
322
395
413
472
710
64
PI-PLC
437
263
TIM alpha/beta barrel
594
B
Myristoylation
X domain
PDZ domain
PI-PLC
C-terminus
TIM alpha/beta barrel
C
EF hand
domains
X-Y linker
X-Y catalytic
domain
C2 domain

Figure 3. Overall structure of *TbPI-PLC-like*.
(A) *T. brucei*'s PI-PLC (*TbPI-PLC*) has a similar domain organization to the mammalian PLC zeta with all the canonical PLC domains, an EF-hand domain (EF), a TIM beta/alpha barrel with an X and a Y catalytic domain, and a C2 domain. In addition, it also has a myristoylation (M) consensus sequence at the N-terminus. In comparison, *TbPI-PLC-like* has a much simpler domain organization. It has the myristoylation consensus sequence at the N-terminus, and a modified TIM beta/alpha barrel with a PDZ domain instead of a Y domain. *TbPI-PLC-like* does not have an EF-hand domain or a C2 domain. Sequence and structural similarities (noted amino acids) place *TbPI-PLC-like* in the PI-PLC family and TIM alpha/beta barrel phosphodiesterase superfamily respectively.
(B) I-TASSER model of *TbPI-PLC-like* is represented in ribbon form with domain boundaries colored as in (A) with the myristoylation consensus sequence (membrane binding region) at the top. Also shown is IP_3 (red, grey and gold spheres) bound to a loop of the PDZ domain in a pocket formed by the X domain, the PDZ domain and rest of the TIM alpha/beta barrel sequence.
(C) Three-dimensional protein structure model for PLC zeta (PDB: Q86YW0) generated by SWISS-MODEL with IP_2 bound to the X-Y catalytic domain.

Figure 4. Sequence alignment of PI-PLC-like proteins.

Alignment of the amino acid sequences of the TIM alpha/beta barrel region of PI-PLC-like proteins of representative Kinetoplastid species is shown. The amino acids corresponding to the TIM alpha/beta barrel are colored in grey, the X domain in yellow, and the PDZ domain in blue. Residues of the PDZ domain predicted to be important for protein binding are bolded.

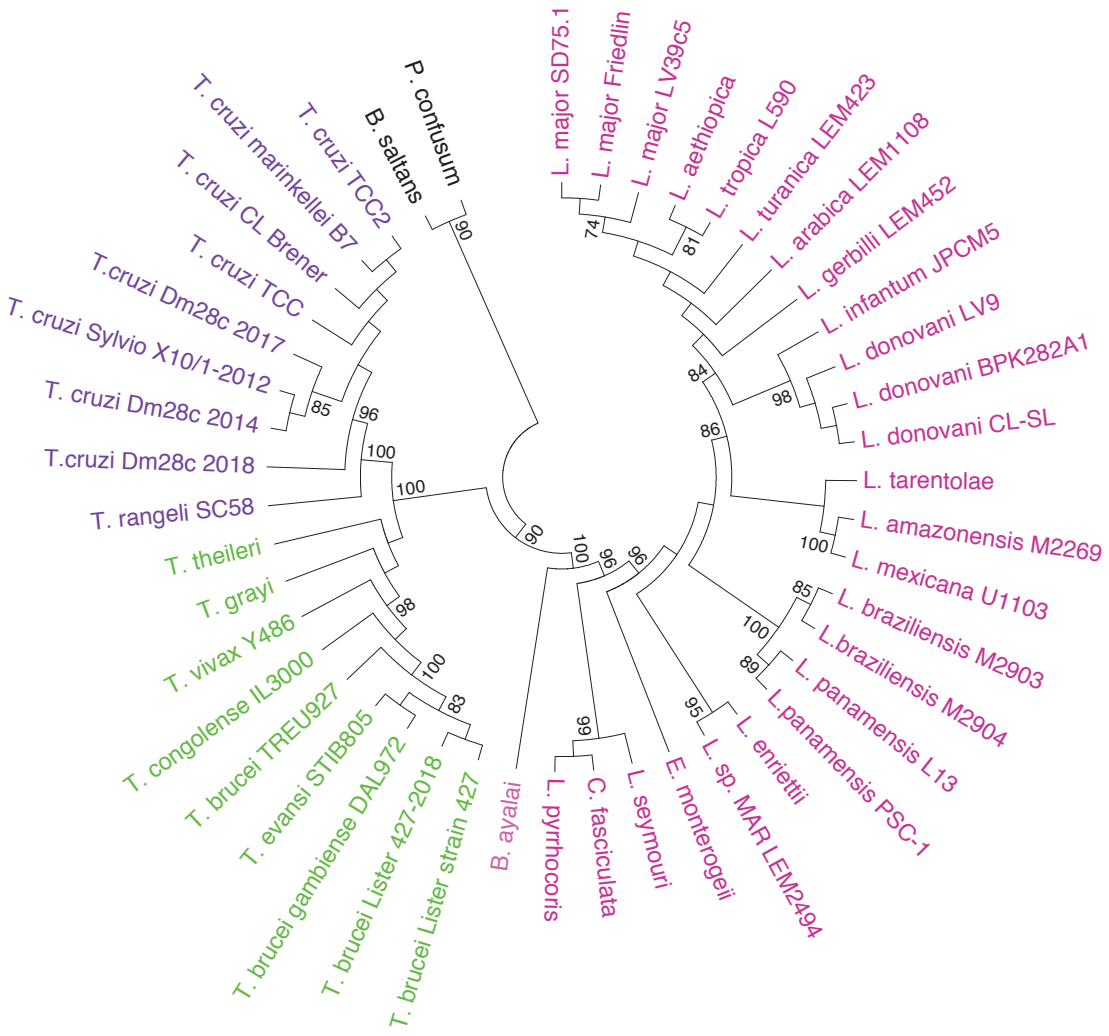

Figure 5. Phylogenetic tree of *TbPI-PLC-like* orthologs.
Maximum likelihood tree showing how orthologs of *TbPI-PLC-like* cluster. The phylogeny was made using PhyML with 1000 bootstrap replicates using the JTT amino acid replacement model. *B. saltans* and *P. confusum* form an outgroup (black). *T. cruzi* isolates cluster together with *T. rangeli* (isolate from Brazil – purple group). The African Trypanosomes form their own group (green). While Leishmania species cluster with other Kinetoplastids (pink).

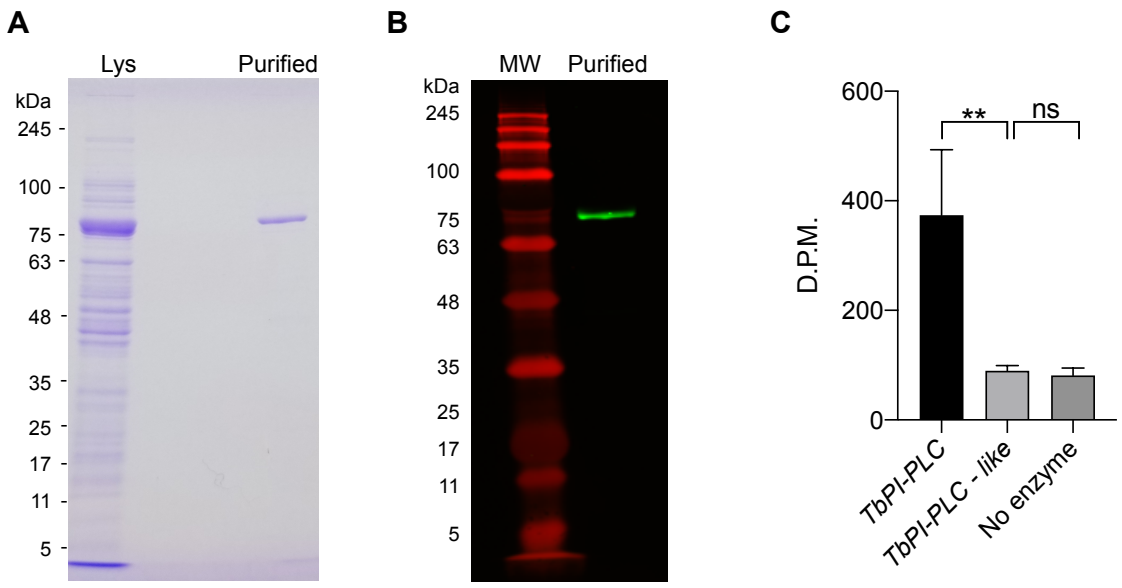

Figure 6. Recombinant *TbPI-PLC-like*.

(A) SDS-PAGE analysis of bacterial lysate after induction (Lys) and desalted fraction (Purified) obtained during *TbPI-PLC-like* affinity purification showing a band at 78.0 kDa.

(B) Western blot analysis of the desalted fraction (Purified) collected during *TbPI-PLC-like* affinity purification, using commercial anti-histidine tag antibodies.

(C) PIP_2 hydrolysis activity assay. *TbPI-PLC* positive control, no enzyme negative control. D.P.M. (disintegrations per minute). Error bars indicate standard deviation from three replicates. One-way ANOVA, (**) p = 0.0061, (ns) p = 0.9874.

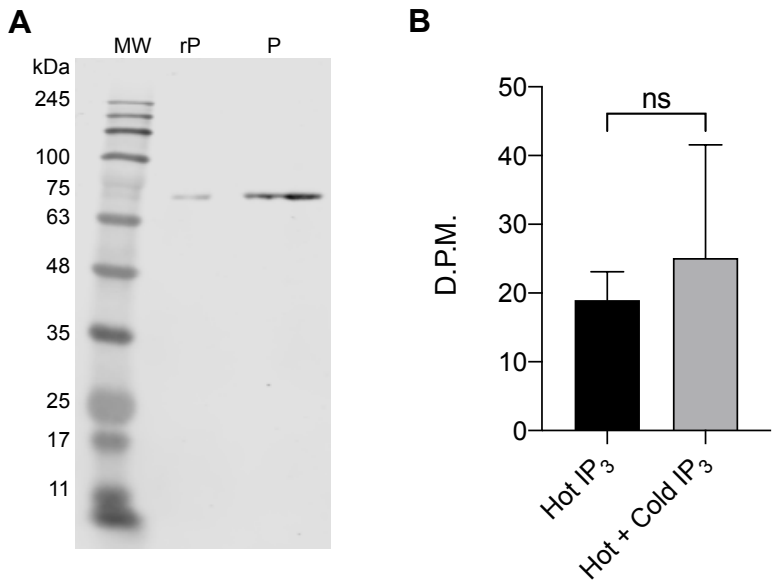

Figure 7. *TbPI-PLC-like* does not bind IP_3 *in vitro*.
(A) Western blot analysis of the recovered pellet (P) fraction of the IP_3 binding assay compared to recombinant *TbPI-PLC-like* (rP) using the affinity purified mouse polyclonal antibodies anti-*TbPI-PLC-like*.
(B) D.P.M. (disintegrations per minute) counts of the pellet fraction of recombinant *TbPI-PLC-like* incubated with ^3H-IP_3 (hot), or ^3H-IP_3 and cold IP_3 (Hot + Cold). Error bars indicate standard deviation from three replicates. Students' *t* test, (ns) p = 0.6026.

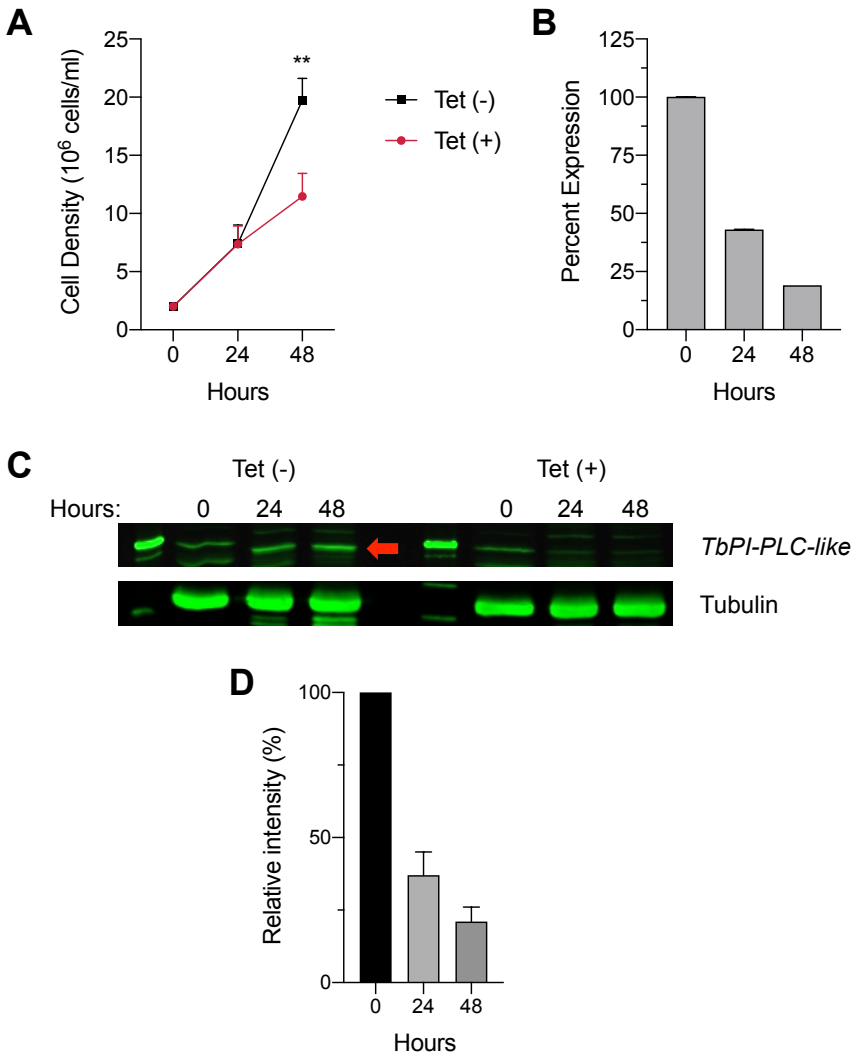

Figure 8. Inhibition of *TbPI-PLC-like* expression by tetracycline inducible RNAi.

(A) Growth PCF trypanosomes in the absence (black squares) or presence (red circles) of 1 μg/ml of tetracycline for 48 hours. Error bars indicate standard deviations from three biological replicates. Students' *t* test, (**) p = 0.006.

(B) Real-time PCR analysis of mRNA expression of *TbPI-PLC-like* at 0, 24 and 48 hours of RNAi. Error bars indicate standard deviation from three biological replicates.

(C) Western blot analyzing the effect of RNAi on *TbPI-PLC-like* protein expression at 0, 24 and 48 hours, using anti *TbPI-PLC-like* polyclonal antibodies. Commercial tubulin antibodies used as a loading control.

(D) Quantification of the intensity of the bands in (C). Comparing the intensity of the *TbPI-PLC-like* bands to that of the Tubulin bands. Error bars indicate standard deviation from three biological replicates.

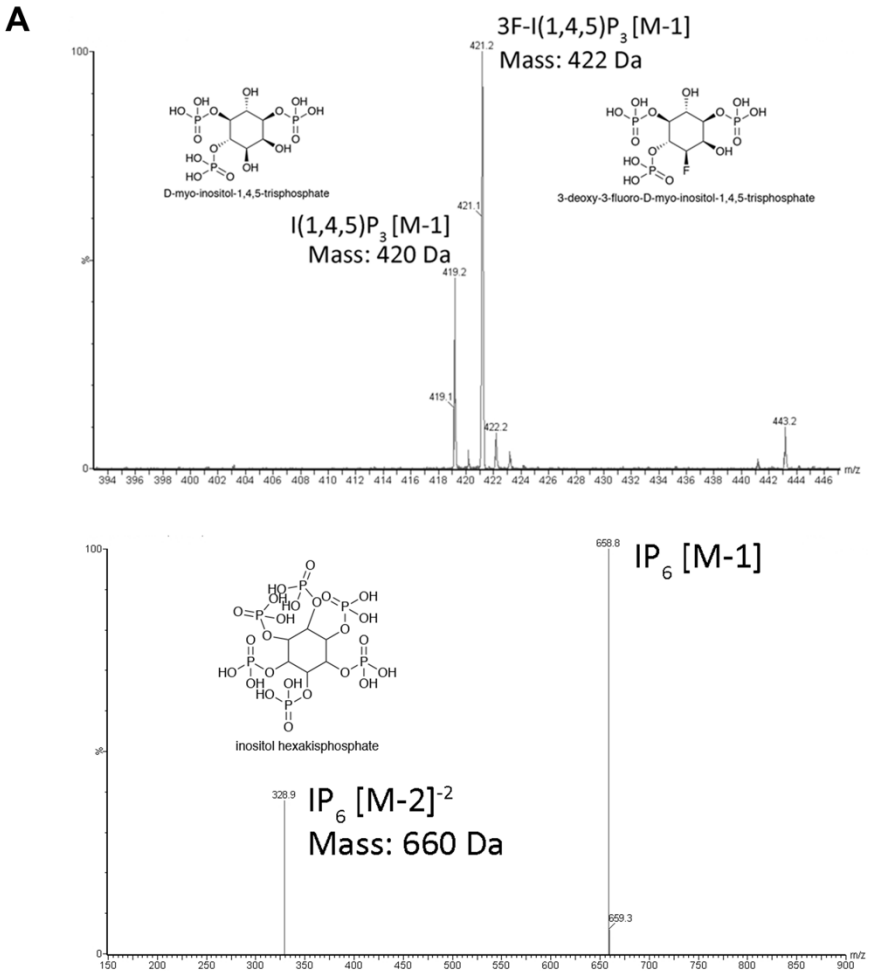
A
3F-I(1,4,5)P3 [M-1]
Mass: 422 Da
421.2
D-myo-inositol-1,4,5-trisphosphate
3-deoxy-3-fluoro-D-myo-inositol-1,4,5-trisphosphate
I(1,4,5)P3 [M-1]
Mass: 420 Da
421.1
419.2
419.1
422.2
443.2
m/z
IP6 [M-1]
658.8
inositol hexakisphosphate
IP6 [M-2]-2
Mass: 660 Da
328.9
659.3
B
n.s.
Relative abundance
Tet (-)
Tet (+)
IP6

Figure 9. LC-MS analysis of Inositol Phosphate abundance in *TbPI-PLC-like* knockdown.

(A) Representative images of mass spectrometry tracings showing peaks at the molecular masses corresponding to various inositol phosphates. Top panel shows the peaks for IP_3 (I(1,4,5)P_3; 420 m/z) and the internal standard 3-fluoro-IP_3 (3F-I(1,4,5)P_3; 422 m/z) as well as the structural formulae (inserts) for both compounds. The bottom panel shows the peak and structural formula for IP_6 (660 m/z).

(B) Bar graphs scaled in arbitrary units and normalized with a standard, 3-fluoro-IP_3, showing the relative abundance of IP_6 measured using mass spectrometry. Error bars indicate standard deviations from three biological replicates. Student's *t* test, (ns) p = 0.765.

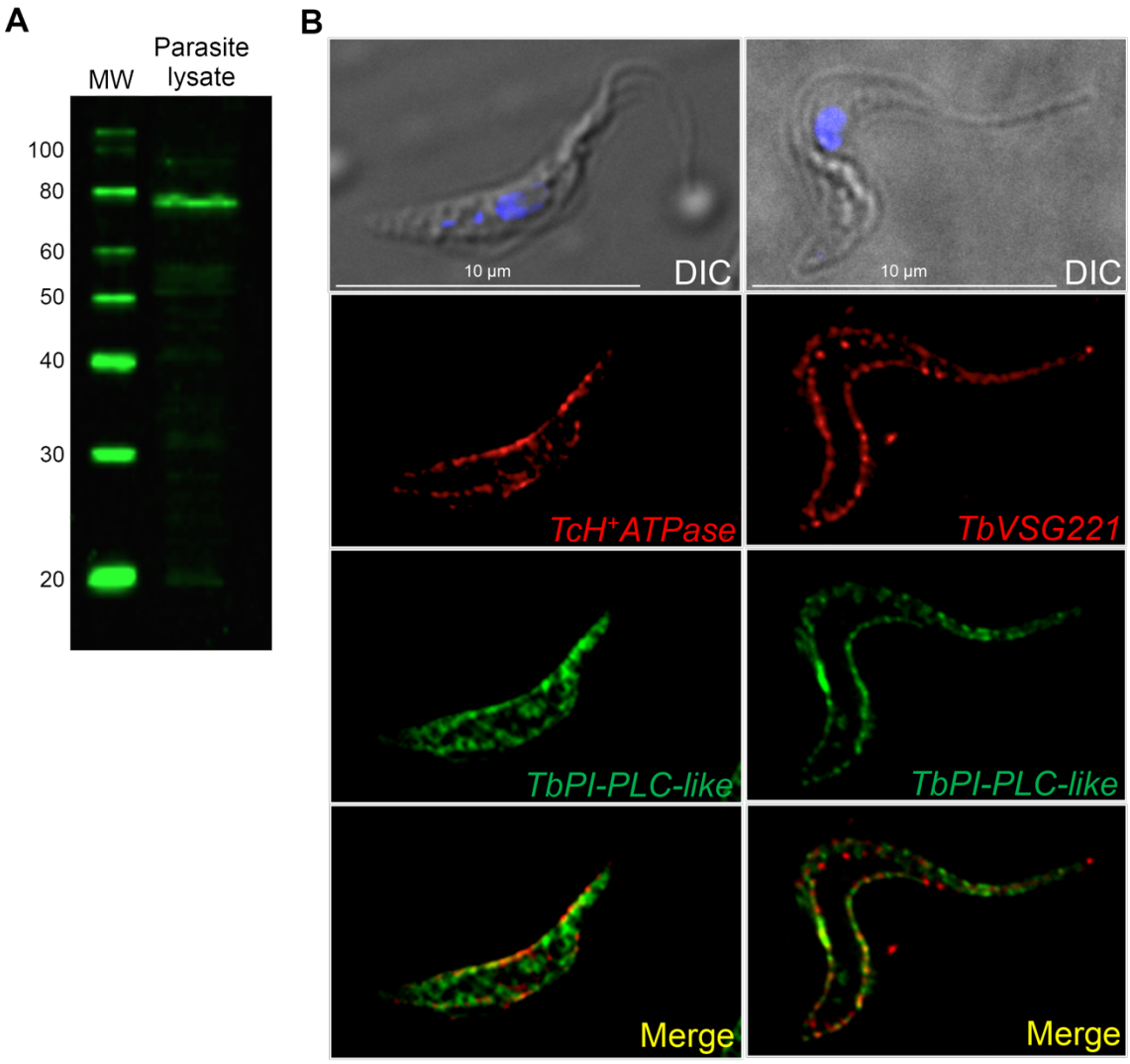

Figure 10. Localization of *TbPI-PLC-like*.
(A) Western blot analysis of total cell lysate from PCF 427 WT *T. brucei* (Parasite lysate), using affinity purified mouse polyclonal antibodies against *TbPI-PLC-like* (1:1,000), showing a band at 78.0 kDa.
(B) Subcellular localization of *TbPI-PLC-like* in PCF (top panels) and BSF (bottom panels) trypanosomes. In PCF *TbPI-PLC-like* colocalizes with the plasma membrane marker *TcH⁺ATPase* (*T. cruzi* proton ATPase) with a Pearson correlation coefficient of 0.8816. It also has a reticulated distribution in the cytosol. In BSF *TbPI-PLC-like* colocalizes with the plasma membrane marker TbVSG221 with a Pearson correlation coefficient of 0.6319. There is less expression in the cytosol as compared to PCF. DIC, differential interference contrast microscopy.

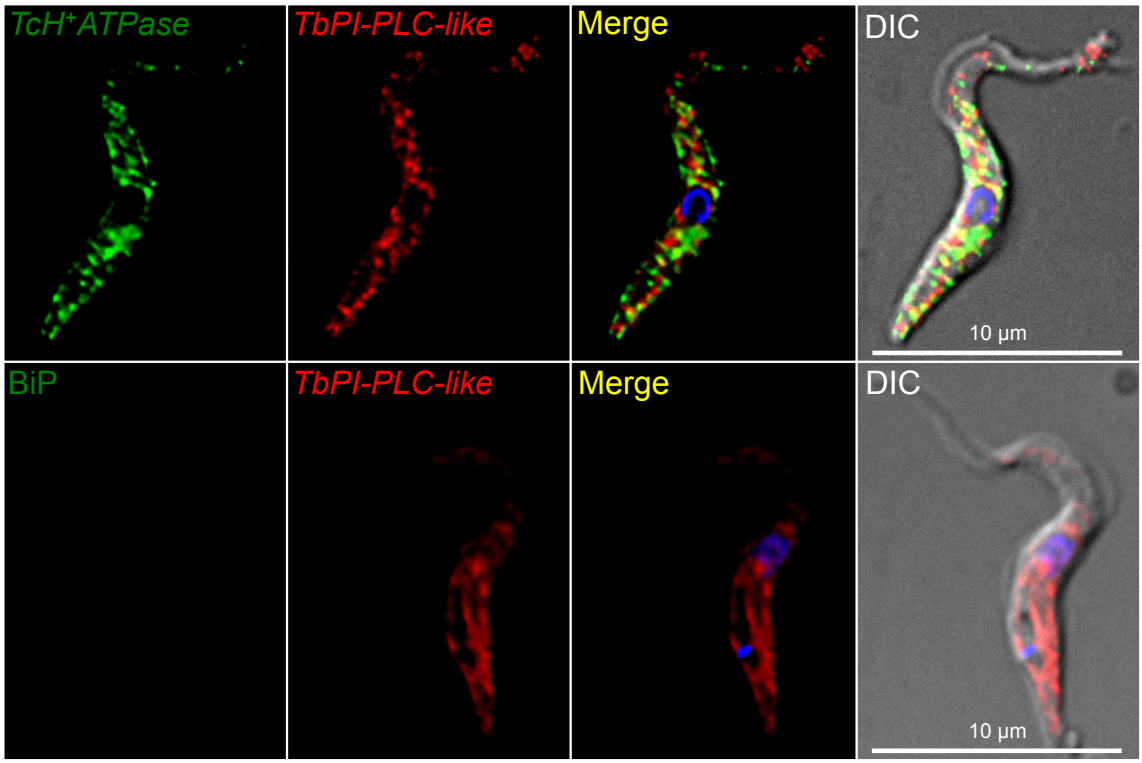

Figure 11. *TbPI-PLC-like* localizes to the outer surface of the plasma membrane in PCF.

Non permeabilized trypanosomes were incubated with the membrane marker *TcH*$^{+}$*ATPase* and the polyclonal *TbPI-PLC-like* antibodies showing a localization to the outer surface of the membrane (top panel). A negative control with BiP (endoplasmic reticulum marker) is shown in the bottom panel.

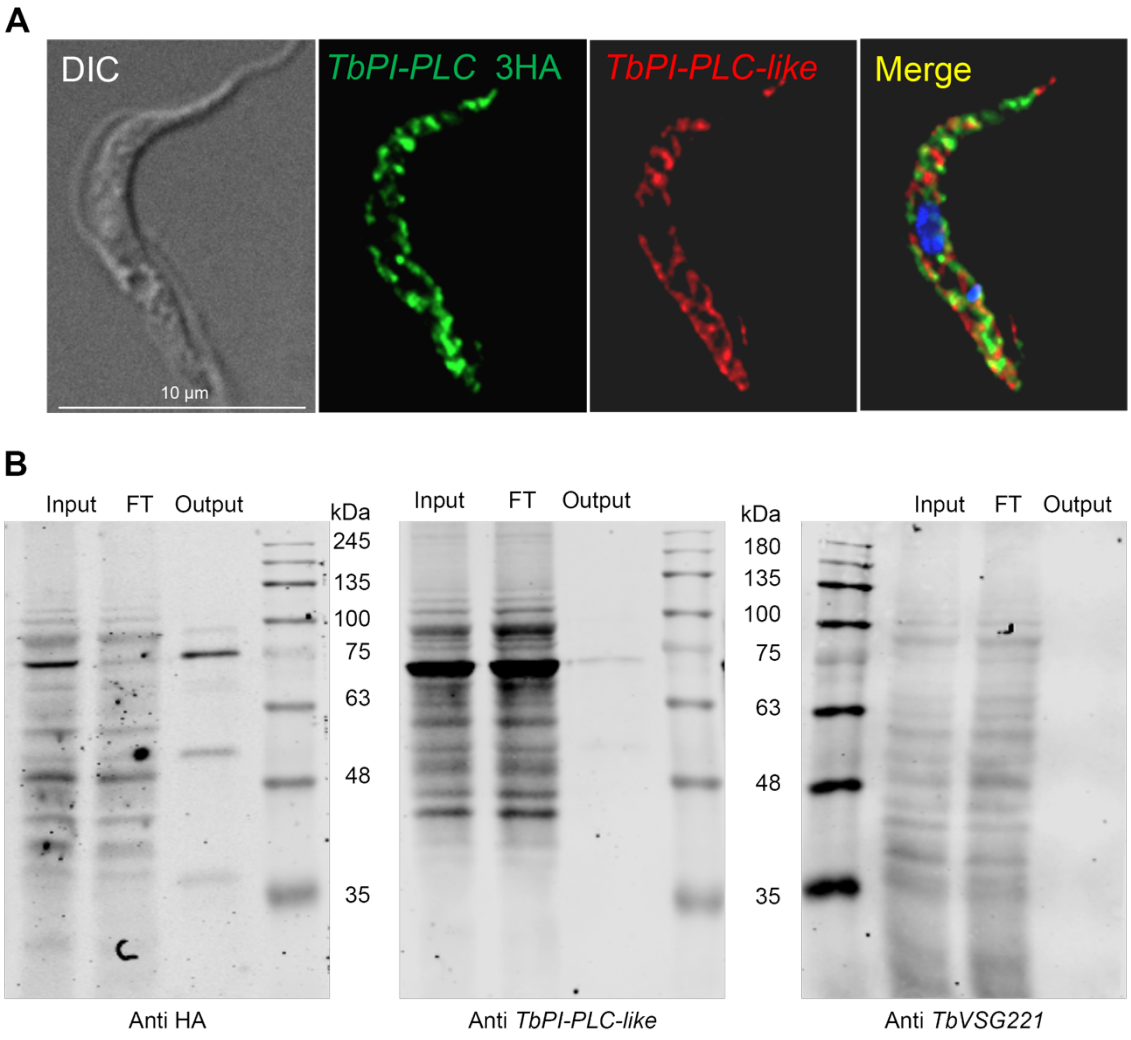

Figure 12. Interaction between *TbPI-PLC* HA and *TbPI-PLC-like*.
(A) HA tagged *TbPI-PLC* and *TbPI-PLC-like* have a similar subcellular localization on the cytoplasm and the plasma membrane. The two proteins partially co-localize, but not fully. Pearson correlation coefficient 0.6574. DIC, differential interference contrast microscopy.
(B) Western blot analysis of *TbPI-PLC* pulldown with anti HA agarose beads, using commercial anti HA antibodies, polyclonal *TbPI-PLC-like* antibodies, and *TbVSG221* antibodies (negative control).

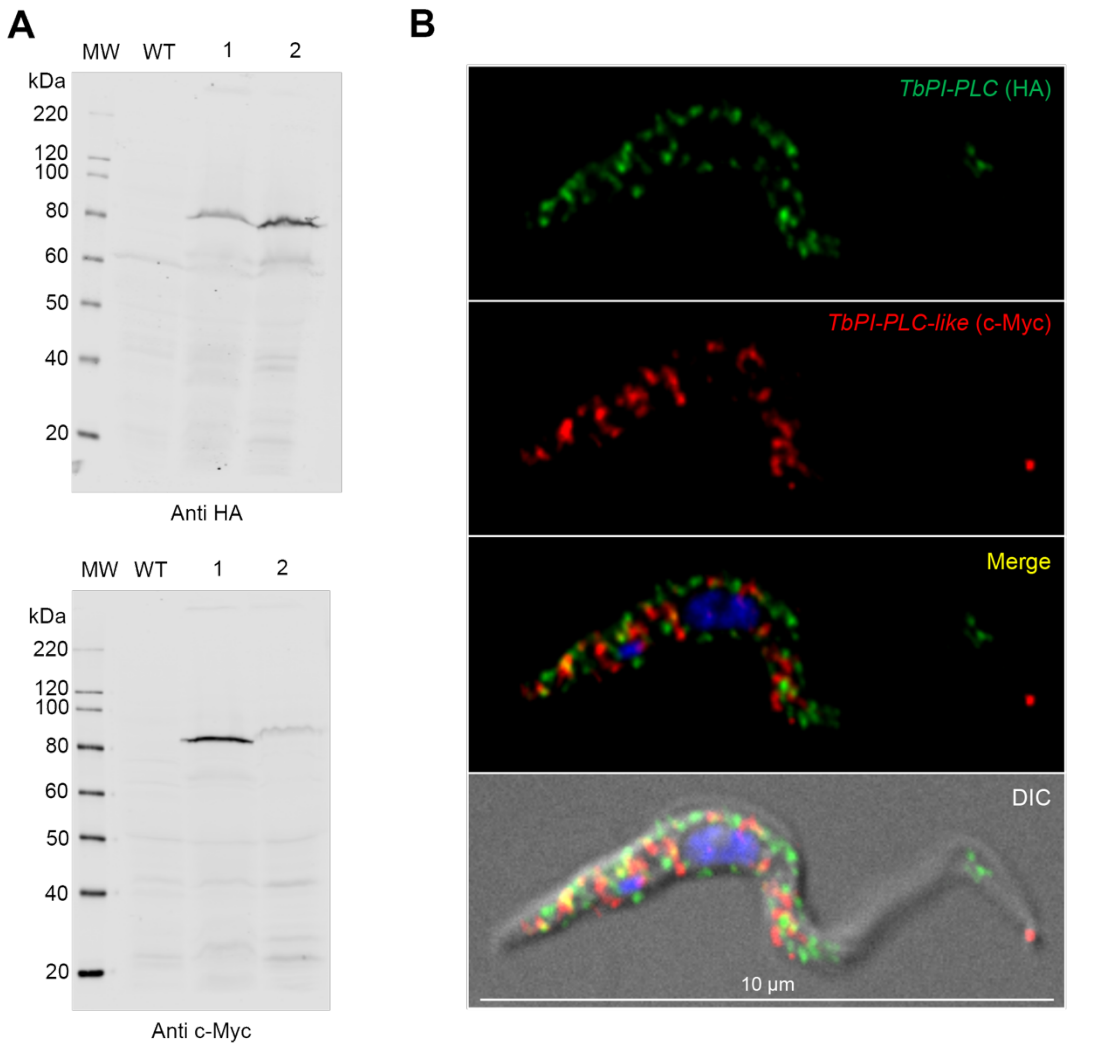
A
MW WT 1 2
kDa
220
120
100
80
60
50
40
20
Anti HA
MW WT 1 2
kDa
220
120
100
80
60
50
40
20
Anti c-Myc
B
TbPI-PLC (HA)
TbPI-PLC-like (c-Myc)
Merge
DIC
10 µm
C
TbPI-PLC HA
TbPI-PLC-like c-Myc
kDa
F T W IP
82
78
78
TbPI-PLC (HA)
TbPI-PLC-like (c-Myc)
TbPI-PLC-like
TbPI-PLC-like HA
TbPI-PLC c-Myc
kDa
F T W IP
78
82
78
TbPI-PLC-like (HA)
TbPI-PLC (c-Myc)
TbPI-PLC-like

Figure 13. Absence of interaction between *TbPI-PLC-like* and *TbPI-PLC* in double tagged cell lines.

(A) Western blot validation of double tagged PCF Trypanosomes. Lane 1: *TbPI-PLC* tagged with HA (82 kDa), *TbPI-PLC-like* tagged with c-Myc (78 kDa). Lane 2: *TbPI-PLC* tagged with c-Myc (82 kDa), *TbPI-PLC-like* tagged with HA (78 kDa). Top panel, commercial anti HA antibody. Bottom panel, commercial anti c-Myc antibody.

(B) Subcellular localization of HA tagged *TbPI-PLC* (green), and c-Myc tagged *TbPI-PLC-like* (red). Both tagged proteins have a punctate distribution in the cytosol and around the plasma membrane. However, they don't co-localize.

(C) Western blot analysis of the pulldown with anti HA agarose beads of *TbPI-PLC* (left hand side panel) and *TbPI-PLC-like* (right hand side panel. Using commercial anti HA and c-Myc antibodies, and the polyclonal anti *TbPI-PLC-like* antibodies. FT - flow through, W - wash, IP - output.

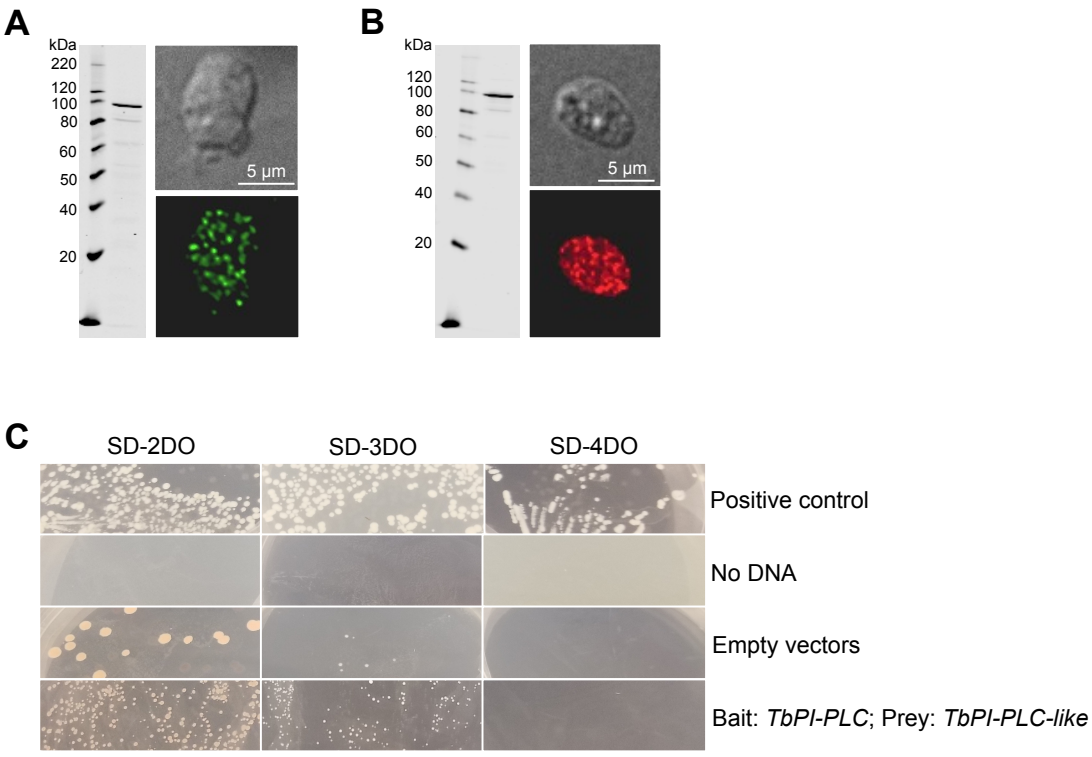

Figure 14. Yeast Two Hybrid Analysis.
(A) Western blot validation of the expression of the bait construct (*TbPI-PLC* in pGBKT7) in the AH109 yeast cell line. Immunofluorescence analysis shows that the protein is expressed in the cytoplasm. Commercial antibodies against c-Myc.
(B) Western blot validation of the expression of the prey construct (*TbPI-PLC-like* in pGADT) in the AH109 yeast cell line. Immunofluorescence analysis shows that the protein is expressed in the cytoplasm. Commercial antibodies against HA.
(C) Growth of the yeast strain AH109 expressing *TbPI-PLC* as bait together with *TbPI-PLC-like* as prey on SD selection agar plates (SD-2DO, SD-3DO, SD-4DO). Transformations with empty vectors or without DNA were added as negative controls. Transformation with control vectors pGBKT7-53 and pGADT7-T (provided with the kit) was used as a positive control.

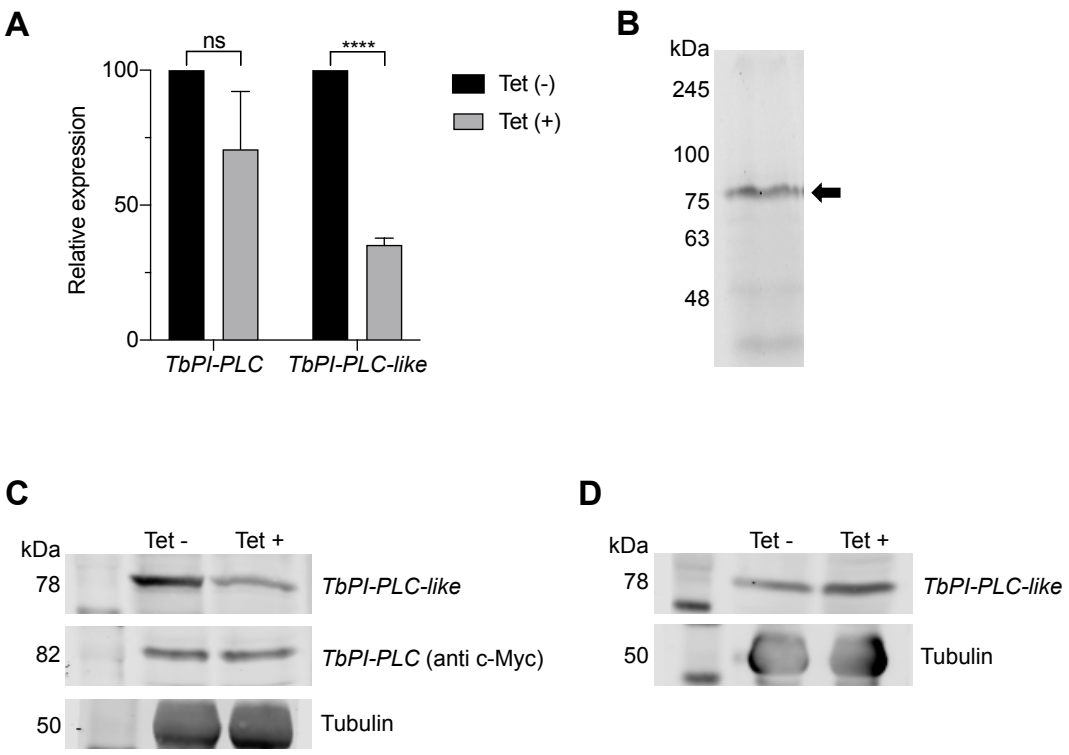

Figure 15. Effect of *TbPI-PLC-like* knockdown by RNAi on the expression of *TbPI-PLC*.

(A) qRT-PCR analysis of gene expression of *TbPI-PLC* and *TbPI-PLC-like* relative to Actin in *T. brucei* PCF grown in presence or absence of tetracycline for 48 hours. Error bars indicate standard deviation from three biological replicates. Students' *t* test, (ns) not significant, (****) p = 0.000002.
(B) Western blot validation of c-Myc tag of *TbPI-PLC* (82 kDa) in a *TbPI-PLC-like* p2T7 cell line. Commercial c-Myc antibodies.
(C) Western blot analysis of protein expression of *TbPI-PLC* and *TbPI-PLC-like* in *T. brucei* PCF (cell line from B) grown in presence or absence of tetracycline for 48 hours. Polyclonal antibodies against *TbPI-PLC-like* and commercial antibodies against c-Myc. Tubulin was used as a loading control.
(D) Western blot analysis of protein expression of *TbPI-PLC* and *TbPI-PLC-like* in *T. brucei* PCF (*TbPI-PLC* p2T7 cell line[29]) grown in presence or absence of tetracycline for 48 hours. Polyclonal antibodies against *TbPI-PLC-like*. Tubulin was used as a loading control.

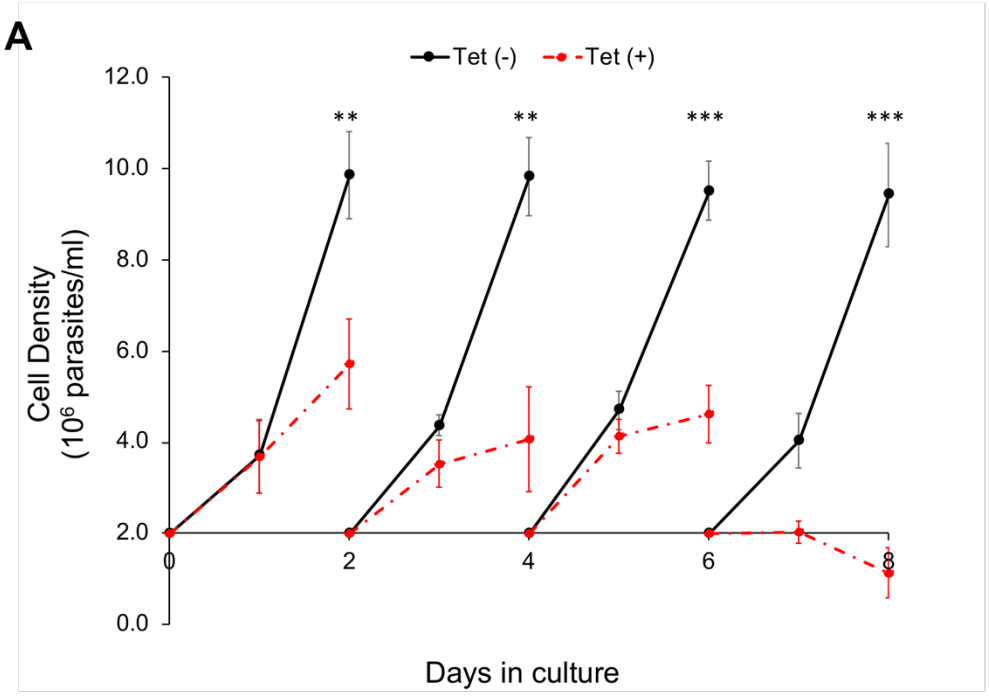
A
Tet (-)
Tet (+)
12.0
10.0
8.0
6.0
4.0
2.0
0.0
Cell Density
(10⁶ parasites/ml)
**
**
***
***
0
2
4
6
8
Days in culture
Tet (-)
Tet (+)
78 kDa
α-TbPI-PLC-like
55 kDa
α-Tubulin

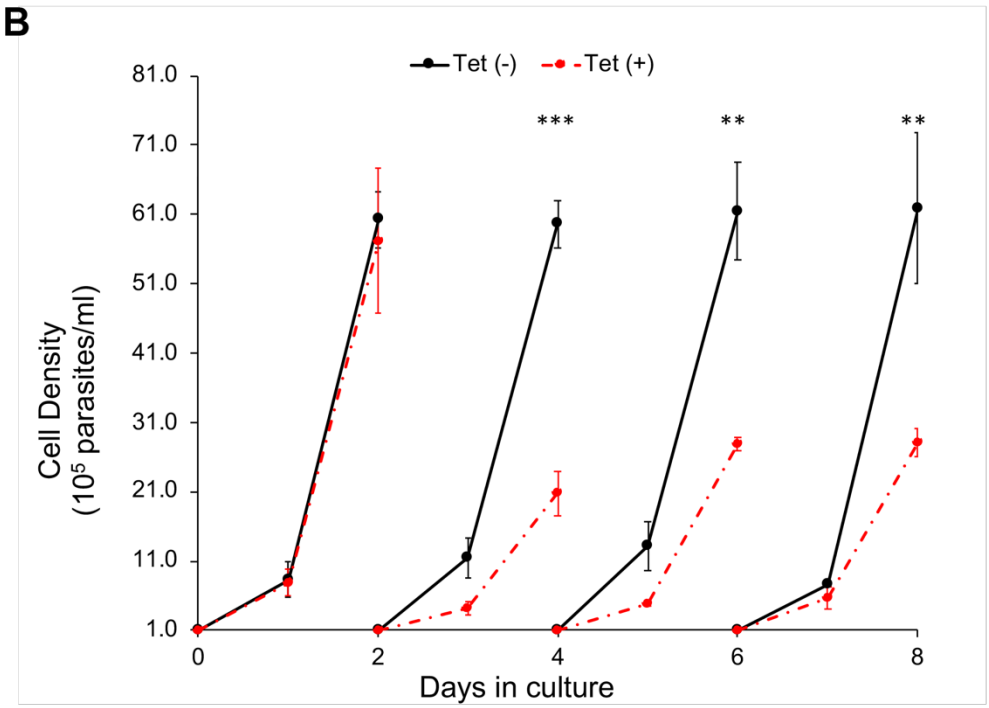
B
Tet (-)
Tet (+)
81.0
71.0
61.0
51.0
41.0
31.0
21.0
11.0
1.0
Cell Density
(10⁵ parasites/ml)
***
**
**
0
2
4
6
8
Days in culture
Tet (-)
Tet (+)
78 kDa
α-TbPI-PLC-like
55 kDa
α-Tubulin

Figure 16. Effect of knockdown of expression of *TbPI-PLC-like* on growth *in vitro*.

(A) *In vitro* growth of PCF 29-13 *TbPI-PLC-like* p2T7 cell line with (red) or without (black) 1 μg/ml tetracycline. Error bars indicate standard deviation of three biological replicates. Students' *t* tests, day 2 (**) p = 0.006, day 4 (**) p = 0.002, day 6 (***) p = 0.0006, day 8 (***) p = 0.0003. Western blot showing the protein expression level of *TbPI-PLC-like* at 48 hours of parasites grown with or without tetracycline. Tubulin used as a loading control.

(B) *In vitro* growth of single marker BSF *TbPI-PLC-like* p2T7 cell line with (red) or without (black) 1 μg/ml tetracycline. Error bars indicate standard deviation of three biological replicates. Students' *t* tests, day 4 (***) p = 0.0001, day 6 (**) p = 0.001, day 8 (**) p = 0.006. Western blot showing the protein expression level of *TbPI-PLC-like* at 48 hours of parasites grown with or without tetracycline. Tubulin used as a loading control.

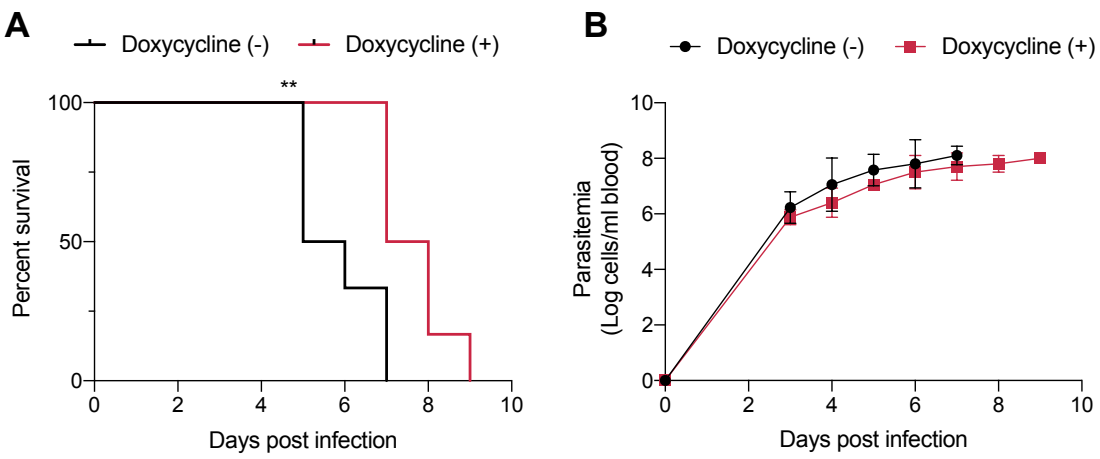

Figure 17. Effect of knockdown of expression of *TbPI-PLC-like* on virulence in mice.

Two groups of six mice were infected with *TbPI-PLC-like* p2T7 BSF trypanosomes. Doxycycline (200 μg/ml) was supplied in the drinking water of one group of mice for the induction of RNA interference of TbPI-PLC-like.

(A) Percentage of mice survival was monitored for nine days until all mice were dead or were euthanized. Log-rank (Mantel-Cox) test (**) p = 0.008, Gehan-Breslow-Wilcoxon test (**) p = 0.009.

(B) Parasitemia levels in the blood of infected mice was monitored for nine days until all mice were dead or were euthanized. Error bars indicate standard deviation.

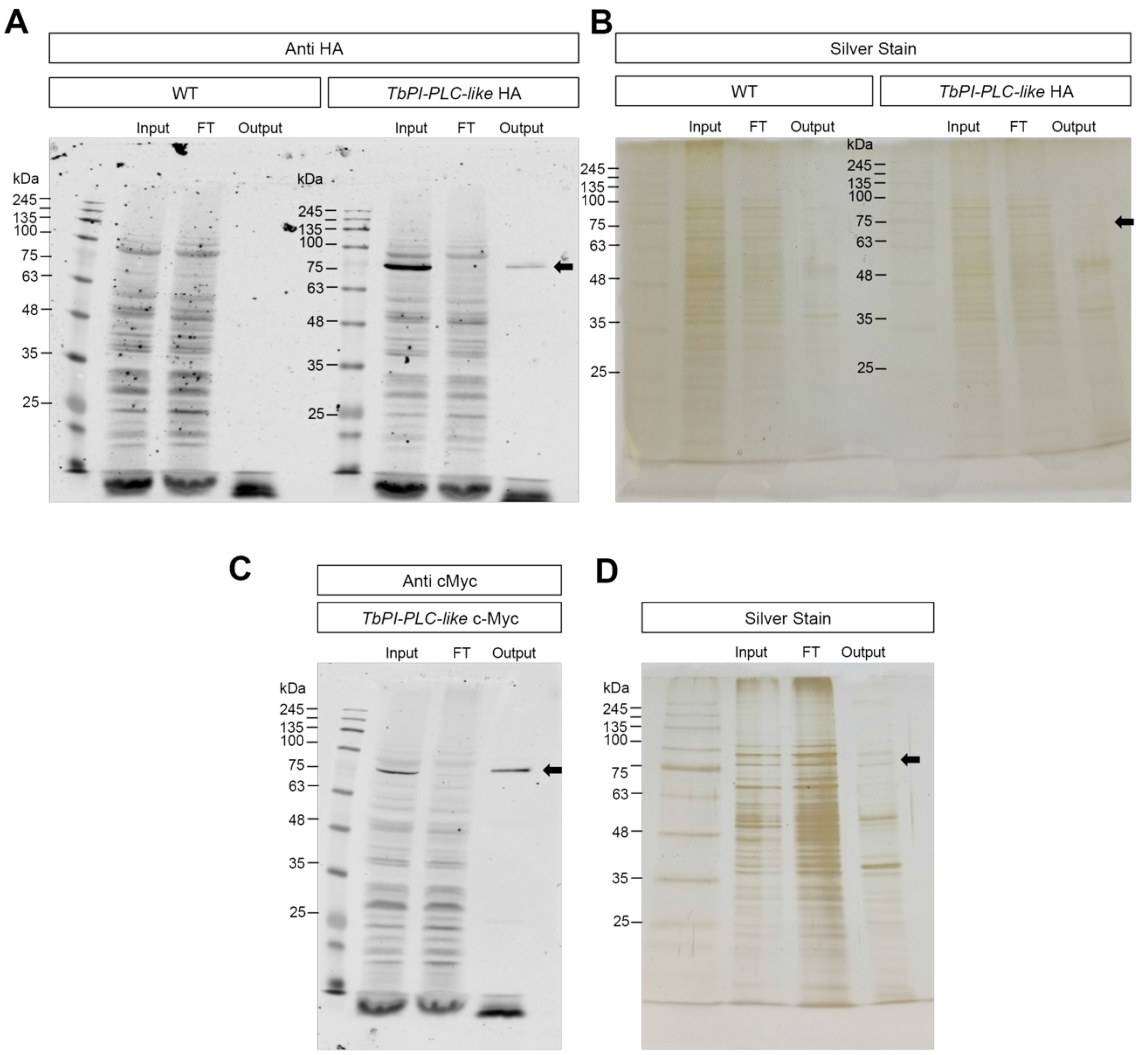

Figure 18. Pull down of endogenously tagged *TbPI-PLC-like* for LC-MS/MS. Wild type and endogenously tagged cell lines were incubated with anti HA (A and B) or anti c-Myc (C and D) magnetic beads for immunoprecipitation. The input, flow through (FT) and output were analyzed by western blot (A and C) and silver stain (B and D). Arrows point to *TbPI-PLC-like* bands.

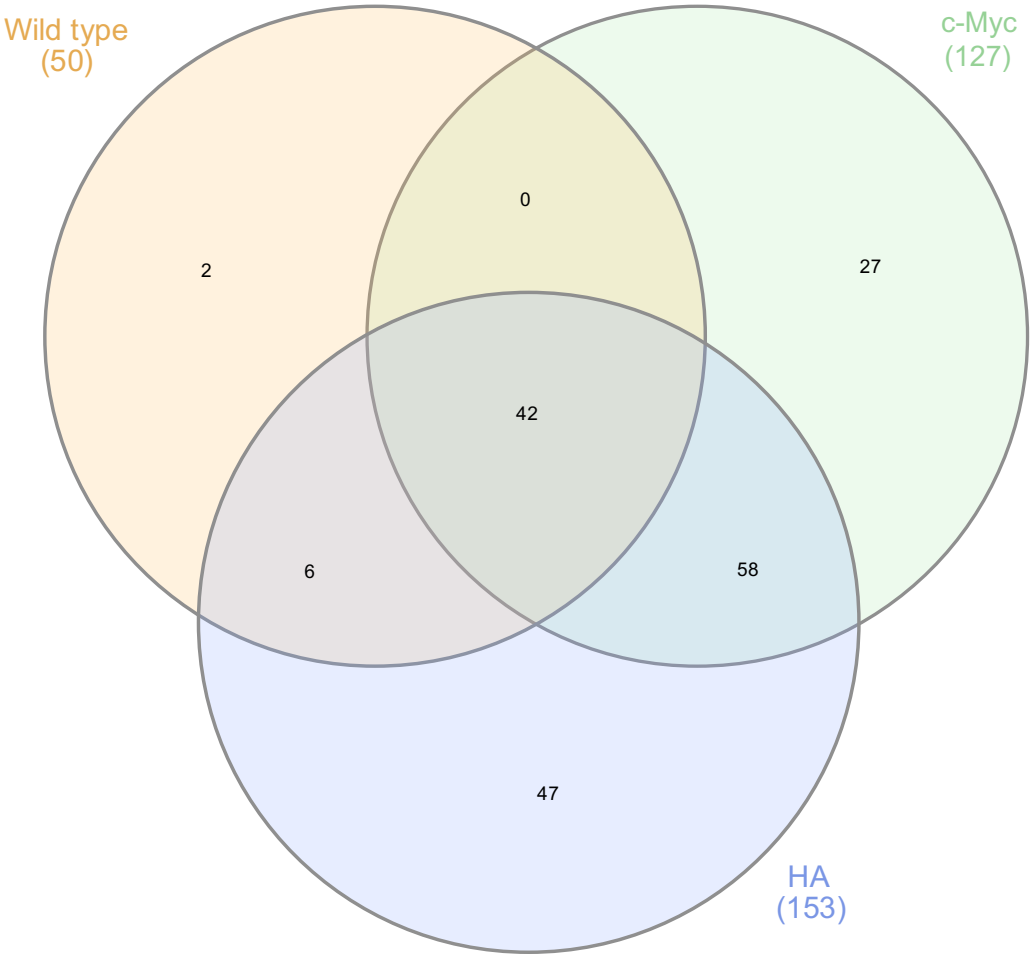

Figure 19. Identification of potential binding partners of *TbPI-PLC-like*.
Proteins pulled down with HA or c-Myc tagged *TbPI-PLC-like*, and from wild type *T. brucei* PCF were analyzed by LC-MS/MS and the results were compared against the TriTrypDB data base to identify the potential binding partners. HA tagged *TbPI-PLC-like* PCFs had 153 binding partners, while c-Myc tagged PCFs had 127 binding partners. The two had 58 binding partners in common that were not pulled down with the wild type PCFs.

Table 1. Primers used in this study.

***TbPI-PLC-like* heterologous expression in pQE-80L vector**	
Forward (*BamHI*)	CGGGATCCGGTTTGTGCAATTCTAAAAG
Reverse (*HindIII*)	CCCAAGCTTTTAGGCCGCCTTGTTCCAGGAAAC
***TbPI-PLC-like* fragment expressed in p2T7^{Ti}B/GFP vector**	
Forward	GGATCCCTCAACGGAAGAAGGTGCTC
Reverse	CCGCGGCCTCCCTCTCTTGAATTCCCG
C-terminal tagging in pMOTag vectors	
TbPI-PLC-like forward	GATACCGCGTTCTGCGCTTGGAGCAGACCGGT GGCCTTACAAGGTTCGACGAGTGCGCACTTGGT GCTCACTGCCTAGTTTCCTGGAACAAGGCGGCC GGTACCGGGCCCCCCCTCGAG
TbPI-PLC-like reverse	TACGCTTACACTCCCGATTGGCAACGCCCGTCG TCACCTAAAACGAGCGGCCTACGTACATTGCGA ATTTGTTAGCATACGTAACGCCATCTCACCCCA CTTGGCGGCCGCTCTAGAACTAGTGGAT
TbPI-PLC forward	TTACGTGCCCTAAAAAAAGGAATTCGCCAGGTC CCCCTTCGAGACCTCAAAGGATCTATTATACAT GGCTCTTTTTTAATGGTTCAAGTATCTTATCAGG GTACCGGGCCCCCCCTCGAG
TbPI-PLC reverse	AGCTACGCTGTGAAGACCATGGCACAACATGGT GCCATAAAGTCGGGTACATGCAACGCACACTTG TAACCCAATTGAAGAACACGATATTCTCAAACTC TGGCGGCCGCTCTAGAACTAGTGGAT
qRT-PCR	
TbActin forward	GTATAGCGTGTGGATTGGCGG
TbActin reverse	TGCTGTGTACGATGCTGGG
TbPI-PLC forward	TGTACGTCACGTGGGCTCTC
TbPI-PLC reverse	GTGCCTCAACTGCCCCTGTC
TbPI-PLC-like forward	TTTGAGAGAGATCAACTAGC
TbPI-PLC-like reverse	CTCGTAAGCCGCCGGGTTCG
Yeast Two Hybrid	
TbPI-PLC-like pGADT7 forward	TATGGCCATGGCCAGTGGGGGAAACCGCTTAA GTG
TbPI-PLC-like pGADT7 reverse	CAGCTCGAGCTCGATGGATCTTAGGCCGCCTT GTTCCAG
TbPI-PLC-like pGBKT7 forward	GCATATGGCCATGGAGGCCGGGGGAAACCGCT TAAGTG
TbPI-PLC-like pGBKT7 reverse	CCGCTGCAGGTCGACGGATCTTAGGCCGCCTT GTTCCAG

TbPI-PLC pGADT7 forward	GCATATGGCCATGGAGGCCGGGCACCGTACCG GCAACC
TbPI-PLC pGADT7 reverse	CCGCTGCAGGTCGACGGATCCTACTGATAAGAT ACTTGAACCATTAAAAAAGAGCCATGTATAATAG
TbPI-PLC pGBKT7 forward	TATGGCCATGGAGGCCAGTGGGCACCGTACCG GCAACC
TbPI-PLC pGBKT7 reverse	CAGCTCGAGCTCGATGGATCCTACTGATAAGAT ACTTGAACCATTAAAAAAGAGCCATGTATAATAG

Table 2. Potential binding partners of *TbPI-PLC-like* – relative abundance.

TriTrypDB I.D.	Protein name	HA R.A.	c-Myc R.A.
Tb427.06.2090	*TbPI-PLC-like*	5.45	4.06
Translation Factors			
Tb427.10.4560	elongation factor 2	1.73	0.28
Tb427.10.13360	elongation factor Tu, putative	0.18	0.17
Tb427tmp.01.3170	activated protein kinase c receptor	0.12	0.16
Ribosomal proteins - 40S			
Tb427.08.6150	40S ribosomal protein S8, putative	1.06	0.43
Tb427.10.14600	40S ribosomal protein S2, putative	0.36	0.40
Tb427tmp.02.4000	40S ribosomal protein S15A, putative	0.33	0.52
Tb427.10.3940	40S ribosomal protein S3A, putative	0.28	0.51
Tb427.10.11540	40S ribosomal protein S3, putative	0.18	0.41
Tb427tmp.01.3020	40S ribosomal protein L14, putative	0.18	0.35
Tb427.03.1370	40S ribosomal protein S25, putative	0.12	0.22
Tb427.10.7330	40S ribosomal protein S24E, putative	0.11	0.40
Ribosomal proteins - 60S			
Tb427.03.3310	60S ribosomal protein L13, putative	0.77	1.26
Tb427.10.11390	60S ribosomal protein L6, putative	0.75	0.49
Tb427tmp.02.4050	60S ribosomal protein L28, putative	0.62	0.66
Tb427.04.2180	60S ribosomal protein L35a, putative	0.59	0.35
Tb427.05.1610	60S ribosomal protein L13a, putative	0.39	0.55
Tb427.08.1330	60S ribosomal protein L7a, putative	0.39	0.35
Tb427.10.13500	60S ribosomal protein L10a	0.31	0.49
Tb427.07.5000	60S ribosomal protein L19, putative	0.30	0.35
Tb427.07.1730	60S ribosomal protein L7, putative	0.30	0.28
Tb427tmp.211.2630	60S ribosomal protein L23, putative	0.27	0.14
Tb427.02.6090	60S ribosomal protein L44	0.23	0.64

Tb427.10.9880	60S ribosomal protein L18, putative	0.21	0.23
Tb427.10.3840	60S ribosomal protein L18a, putative	0.18	0.30
Tb427tmp.46.0002	60S acidic ribosomal subunit protein, putative	0.15	0.22
Tb427tmp.211.0110	60S ribosomal protein L10, putative	0.13	0.40
Tb427.07.5170	60S ribosomal protein L23a	0.12	0.18
Ribosomal proteins - mitochondrial			
Tb427.04.1800	ribosomal protein L3, mitochondrial, putative	0.32	0.50
Ribosomal proteins			
Tb427.04.1100	ribosomal protein L21E (60S), putative	0.23	0.53
Tb427tmp.160.2490	ribosomal protein S7, putative	0.11	0.77
Tb427.10.1590	ribosomal protein L36, putative	0.10	0.72
TCA cycle			
Tb427.10.7410	succinyl-CoA ligase (GDP-forming) beta-chain, putative	0.78	0.19
Tb427tmp.01.1740	2-oxoglutarate dehydrogenase E1 component, putative	0.39	0.12
Heat Shock proteins			
Tb427.07.710	heat shock 70 kDa protein, putative	0.62	0.23
Tb427tmp.02.5450	glucose-regulated protein 78, putative	0.46	0.14
Mitochondrial proteins			
Tb427.10.14820	ADP/ATP translocase 1, putative	0.55	0.18
Tb427.05.1060	metallo-peptidase, Clan ME, Family M16	0.28	0.24
S-adenosylmethionine synthetase			
Tb427.06.4840	S-adenosylmethionine synthetase, putative	0.49	0.05
Retrotransposon Hot Spot proteins			
H25N7.12:mRNA	retrotransposon hot spot protein, RHS4	0.47	0.87
Tb427.02.470	retrotransposon hot spot protein 4 (RHS4), putative	0.47	0.87
Tb427.02.450	retrotransposon hot spot protein 4 (RHS4), putative	0.47	0.87
Tb427.02.1120	retrotransposon hot spot protein 4 (RHS4), point mutation	0.28	0.33

Tb427.02.270	retrotransposon hot spot protein 3 (RHS3), frameshift	0.10	0.12
Antioxidant			
Tb427tmp.160.4250	tryparedoxin peroxidase	0.45	0.43
EF hand domain			
Tb427.10.3900	protein kinase, putative	0.34	0.12
RNA binding proteins			
Tb427tmp.01.5570	RNA-binding protein	0.32	0.52
Tb427.10.14550	ATP-dependent DEAD/H RNA helicase, putative	0.24	0.33
Tb427.10.3990	DHH1	0.17	0.20
Tb427.06.2550	RNA-binding protein, putative	0.12	0.15
Glycosomal proteins (Glycolysis)			
Tb427.05.930	NADH-dependent fumarate reductase	0.27	0.16
Tb427.10.2010	hexokinase	0.26	0.14
Cell Cycle Regulation			
Tb427.02.4510	cdc2-related kinase, putative	0.26	0.31
Nuclear Import Regulation			
Tb427.06.2640	importin alpha subunit, putative	0.16	0.07
Hypothetical Proteins			
Tb427tmp.211.1800	hypothetical protein, conserved	0.64	0.34
Tb427.02.2510	hypothetical protein, conserved	0.35	0.17
Tb427tmp.46.0009	hypothetical protein, conserved	0.17	0.16
Tb427.06.4770	hypothetical protein, conserved	0.14	0.21

Table 3. Potential binding partners of *TbPI-PLC-like* – Mascot score.

TriTrypDB I.D.	Protein name	HA M.S.	c-Myc M.S.
Tb427.06.2090	*TbPI-PLC-like*	291.93	347.47
Heat Shock proteins			
Tb427tmp.01.3110	heat shock protein 70	573.37	280.61
Tb427.06.3740	heat shock 70 kDa protein, mitochondrial precursor, putative	516.37	221.00
Tb427tmp.02.5450-t26_1-p1	glucose-regulated protein 78, putative	53.30	53.12
Translation Factors			
Tb427.10.4560	elongation factor 2	523.90	171.33
Tb427tmp.01.3170	activated protein kinase c receptor	86.05	65.65
Retrotransposon Hot Spot proteins			
H25N7.12:mRNA	retrotransposon hot spot protein, RHS4	237.63	393.03
Tb427.02.450	retrotransposon hot spot protein 4 (RHS4), putative	196.75	334.81
Tb427.02.470	retrotransposon hot spot protein 4 (RHS4), putative	171.78	356.67
Tb427.02.1120	retrotransposon hot spot protein 4 (RHS4), point mutation	78.59	111.59
Ribosomal proteins - 60S			
Tb427.03.3310	60S ribosomal protein L13, putative	205.23	192.89
Tb427.10.14580	60S ribosomal protein L17, putative	124.55	261.50
Tb427tmp.01.7535	60S ribosomal protein L27, putative	122.20	141.10
Tb427.05.1610	60S ribosomal protein L13a, putative	119.03	68.29
Tb427.04.2180	60S ribosomal protein L35a, putative	118.63	117.57
Tb427.07.5170	60S ribosomal protein L23a	101.79	80.06
Tb427.10.11390	60S ribosomal protein L6, putative	95.61	92.60
Tb427tmp.211.0110	60S ribosomal protein L10, putative	77.77	60.74
Tb427.10.13500	60S ribosomal protein L10a	76.33	68.15
Tb427.07.5000	60S ribosomal protein L19, putative	59.24	137.96
Tb427.10.1100	60S ribosomal protein L9, putative	58.51	40.66
Tb427.10.3840	60S ribosomal protein L18a, putative	49.74	117.23
Tb427.03.5050	60S ribosomal protein L4	49.40	118.29
Tb427.10.9800	60S ribosomal protein L22	47.69	44.20
Ribosomal proteins - 40S			
Tb427tmp.244.2630	40S ribosomal protein S6, putative	120.59	274.33
Tb427.10.3940	40S ribosomal protein S3A, putative	110.49	180.24
Tb427tmp.02.4000	40S ribosomal protein S15A, putative	107.95	92.79
Tb427tmp.01.3020	40S ribosomal protein L14, putative	86.76	71.22
Tb427.10.560	40S ribosomal proteins S11, putative	86.19	114.08
Tb427tmp.02.4170	40S ribosomal protein S5, putative	63.21	108.40

Tb427.10.14600	40S ribosomal protein S2, putative	62.81	46.75
Tb427.06.4980	40S ribosomal protein S14	62.18	91.95
Ribosomal proteins - mitochondrial			
Tb427.04.1800	ribosomal protein L3, mitochondrial, putative	104.04	107.30
Ribosomal proteins			
Tb427tmp.160.2490	ribosomal protein S7, putative	61.99	127.17
Tb427.04.1100	ribosomal protein L21E (60S), putative	59.96	151.34
TCA cycle			
Tb427tmp.01.3550	2-oxoglutarate dehydrogenase E2 component, putative	147.75	107.01
Tb427.10.7410	succinyl-CoA ligase (GDP-forming) beta-chain, putative	56.39	48.61
EF hand domain			
Tb427.10.3900	protein kinase, putative	133.53	43.87
RNA binding proteins			
Tb427.10.14550	ATP-dependent DEAD/H RNA helicase, putative	130.69	158.35
Tb427tmp.01.5570	RNA-binding protein	54.70	156.21
Tb427.06.2550	RNA-binding protein, putative	45.88	52.61
Tb427.10.3990	DHH1	45.57	64.66
Mitochondrial proteins			
Tb427.10.14820	ADP/ATP translocase 1, putative	116.36	90.76
Tb427.05.1060	metallo-peptidase, Clan ME, Family M16	67.69	91.19
Antioxidant			
Tb427tmp.160.4250	tryparedoxin peroxidase	86.04	94.43
Nuclear Import Regulation			
Tb427.06.2640	importin alpha subunit, putative	79.97	67.87
Glycosomal proteins (Glycolysis)			
Tb427.05.930	NADH-dependent fumarate reductase	79.58	72.45
Tb427.10.2010	hexokinase	45.67	40.43
Hypothetical proteins			
Tb427tmp.211.1800	hypothetical protein, conserved	193.07	164.98
Tb427.02.2510	hypothetical protein, conserved	67.91	73.35
Tb427tmp.46.0009	hypothetical protein, conserved	44.58	75.88

CHAPTER 3

CONCLUSIONS AND FUTURE DIRECTIONS

Calcium is an essential second messenger for trypanosomatids. Cytosolic free calcium concentration is in the range of 20-100 nM[32]. Signaling begins when calcium levels rise in the cytoplasm. Calcium is acquired from the extracellular environment probably through a putative voltage-gated calcium channel that localizes to the flagellum[135]. A plasma membrane calcium ATPase (PMCA) is responsible for exporting cytosolic calcium, therefore regulating steady-state levels[136]. In addition to exchanging calcium with the extracellular environment, trypanosomatids also store calcium in various organelles that can be mobilized for signaling when necessary[39]. The sarcoplasmic-endoplasmic reticulum (SERCA)-type calcium ATPase in involved in the uptake by the endoplasmic reticulum[137]. Trypanosomatids have a mitochondrial calcium uniporter (MCU) for calcium uptake[138] and efflux is possibly due to a calcium proton exchanger. The acidocalcisome is the main calcium store in trypanosomes. A PCMA-type calcium-proton countertransporting ATPase is responsible for uptake[139] into the acidocalcisome and release is via the IP3 receptor[36]. Membrane contact sites between the acidocalcisome and the mitochondrion[41] might facilitate the transfer of calcium between these two organelles. *T. brucei* has a PI-PLC that hydrolyzes PIP_2 generating IP_3[29]. However, this protein was found to be active at cytosolic

calcium levels suggesting that there might be another way to regulate its activity or the availability of IP_3 in *T. brucei*. This project explored the possibility that a paralogous protein, a PI-PLC-like, was fulfilling that role.

Sequence and structural analysis of *TbPI-PLC-like* revealed that the protein does not have a full catalytic domain and was therefore predicted to be a pseudoenzyme. In addition, *TbPI-PLC-like* has a PDZ domain suggesting that it could be involved in protein-protein or protein-phosphoinositide interactions. This suggestion was reinforced by the prediction that the PDZ domain might bind to IP_3 by the I-TASSER structural modelling server, and by the fact that *TbPI-PLC-like* was pulled down with IP_4 beads[84]. However, recombinant *TbPI-PLC-like* did not bind to IP_3 *in vitro* and knockdown did not have an effect on the total amount of IP_6 in the cell, suggesting that the protein does not directly regulate the inositol phosphate pathway.

We investigated the relationship of *TbPI-PLC-like* and *TbPI-PLC* and got mixed results. There seems to a be a weak or indirect interaction between the two proteins, as *TbPI-PLC-like* is consistently pulled down with HA tagged *TbPI-PLC* and the two proteins have partial colocalization *in vivo*. However, this interaction completely went away when the two proteins were tagged. To directly test whether there is a regulatory relationship between the two proteins we looked at their expression when the reciprocal gene was knocked down. The expression of *TbPI-PLC* is not affected by the knockdown of *TbPI-PLC-like*, and the expression of *TbPI-PLC-like* is not affected by the knockdown of *TbPI-PLC*. These results strongly suggest that *TbPI-PLC-like* does not regulate the activity of *TbPI-PLC*.

We confirmed that *TbPI-PLC-like* is not an active enzyme. This pseudoenzyme is unique to Kinetoplastids and highly conserved in the class from the free-living *Bodo saltans* to the parasitic trypanosomatids, suggesting that it has an important function in these organisms. Knockdown resulted in a severe growth defect in PCF and milder, but still significant, growth phenotype in BSF. In PCF *TbPI-PLC-like* is localized to the cytosol and the plasma membrane, in BSF it is mostly in the plasma membrane. We also found that it localizes to the outside of the plasma membrane of PCF.

In order to investigate the possible binding partners of *TbPI-PLC-like* we did a mass spectrometry analysis of the proteins that co-immunoprecipitated with it in two independent experiments. Preliminary analysis of the results seems to confirm that it does not interact with *TbPI-PLC* or the other proteins involved in the metabolism of inositol phosphates, as none of these were pulled down. The most abundant proteins pulled down in both experiments were translation factors and ribosomal proteins, RNA-binding proteins that are involved in translation were also pulled down, but were less abundant. Mitochondrial proteins, most of them involved in respiration, were also very abundant. These were followed by heat-shock proteins and one anti-oxidant protein. A group of retrotransposon hot spot proteins had high abundance, especially in one experiment. Analysis of the Mascot scores of the two experiments revealed similar patterns to the analysis of protein abundance (described above). A quick first step to begin the validation of these results would be to check if *TbPI-PLC-like* colocalizes with mitochondrial, ER and

glycosomal markers by immunofluorescence microscopy. A yeast two hybrid *T. brucei* library screen could also confirm or dismiss some of these interactions.

Proteins involved in protein generation, folding and degradation, together with proteins involved in glycolysis are the most abundant proteins in cells[140]. Therefore, it is necessary to interpret our results with caution and to validate these possible interactions with experimental work. Among the proteins with highest abundance and Mascot scores were HSP70s and protein elongation factors. These two groups of proteins assist in protein folding. So, there is a possibility that *TbPI-PLC-like* acts as a chaperone, assisting in protein folding, this would explain its association with a wide variety of proteins. This hypothesis could be tested by analysis of the association of *TbPI-PLC-like* with nascent proteins incorporating a radioactive amino acid.

Another interesting avenue to investigate is the role of the plasma membrane localization of *TbPI-PLC-like*. If the extracellular localization is confirmed in BSF, this would mean that *TbPI-PLC-like* could be an exposed antigen and that might have clinical relevance. The *T. cruzi* PI-PLC that plays a role in the differentiation of trypomastigotes to amastigotes, is lipid modified at the N-terminus and targeted to the plasma membrane where it stimulates hydrolysis of the host PIP_2[28]. The targeting of the *TcPI-PLC* to the plasma membrane is important for its function. The *T. brucei* GPI-PLC is also targeted to the outer surface of the plasma membrane in a reversible fashion via lipid modifications, where it cleaves the GPI anchor of VSG proteins[56]. It would be interesting to see if the same, a function dependent on it being at the plasma membrane, is true for

the *TbPI-PLC-like*. Expression of the N-terminus of *TbPI-PLC-like* fused to GFP would confirm that it is sufficient for the plasma membrane localization. Mutagenesis studies would then tell us which lipid modifications are involved and are important. The expression of a truncated *Tb-PI-PLC-like* without the N-terminus, would confirm that these lipid modifications are necessary for plasma membrane localization. Generation of a *TbPI-PLC-like* conditional knockout expressing an ectopic copy without the first 20 amino acids would elucidate whether the plasma membrane localization is essential for the function of the protein.

REFERENCES

1 Stevens, J. R., Noyes, H. A., Dover, G. A. & Gibson, W. C. The ancient and divergent origins of the human pathogenic trypanosomes, Trypanosoma brucei and T. cruzi. *Parasitology* **118 (Pt 1)**, 107-116, doi:10.1017/s0031182098003473 (1999).

2 Kaufer, A., Ellis, J., Stark, D. & Barratt, J. The evolution of trypanosomatid taxonomy. *Parasit Vectors* **10**, 287, doi:10.1186/s13071-017-2204-7 (2017).

3 Franco, J. R., Simarro, P. P., Diarra, A. & Jannin, J. G. Epidemiology of human African trypanosomiasis. *Clin Epidemiol* **6**, 257-275, doi:10.2147/CLEP.S39728 (2014).

4 Brun, R., Blum, J., Chappuis, F. & Burri, C. Human African trypanosomiasis. *Lancet* **375**, 148-159, doi:10.1016/S0140-6736(09)60829-1 (2010).

5 Babokhov, P., Sanyaolu, A. O., Oyibo, W. A., Fagbenro-Beyioku, A. F. & Iriemenam, N. C. A current analysis of chemotherapy strategies for the treatment of human African trypanosomiasis. *Pathog Glob Health* **107**, 242-252, doi:10.1179/2047773213Y.0000000105 (2013).

6 Steverding, D. The history of African trypanosomiasis. *Parasit Vectors* **1**, 3, doi:10.1186/1756-3305-1-3 (2008).

7 Serricchio, M. & Butikofer, P. Trypanosoma brucei: a model micro-organism to study eukaryotic phospholipid biosynthesis. *FEBS J* **278**, 1035-1046, doi:10.1111/j.1742-4658.2011.08012.x (2011).

8 Roditi, I. & Lehane, M. J. Interactions between trypanosomes and tsetse flies. *Curr Opin Microbiol* **11**, 345-351, doi:10.1016/j.mib.2008.06.006 (2008).

9 Fenn, K. & Matthews, K. R. The cell biology of Trypanosoma brucei differentiation. *Curr Opin Microbiol* **10**, 539-546, doi:10.1016/j.mib.2007.09.014 (2007).

10 Schneider, A. Unique aspects of mitochondrial biogenesis in trypanosomatids. *Int J Parasitol* **31**, 1403-1415, doi:10.1016/s0020-7519(01)00296-x (2001).

11 Cohen, P. The origins of protein phosphorylation. *Nat Cell Biol* **4**, E127-130, doi:10.1038/ncb0502-e127 (2002).

12 Vlastaridis, P. *et al.* The Pivotal Role of Protein Phosphorylation in the Control of Yeast Central Metabolism. *G3 (Bethesda)* **7**, 1239-1249, doi:10.1534/g3.116.037218 (2017).

13 Livermore, T. M., Azevedo, C., Kolozsvari, B., Wilson, M. S. & Saiardi, A. Phosphate, inositol and polyphosphates. *Biochem Soc Trans* **44**, 253-259, doi:10.1042/BST20150215 (2016).

14 Rao, N. N., Gomez-Garcia, M. R. & Kornberg, A. Inorganic polyphosphate: essential for growth and survival. *Annu Rev Biochem* **78**, 605-647, doi:10.1146/annurev.biochem.77.083007.093039 (2009).

15 Cordeiro, C. D., Saiardi, A. & Docampo, R. The inositol pyrophosphate synthesis pathway in Trypanosoma brucei is linked to polyphosphate synthesis in acidocalcisomes. *Mol Microbiol* **106**, 319-333, doi:10.1111/mmi.13766 (2017).
16 York, J. D. Regulation of nuclear processes by inositol polyphosphates. *Biochim Biophys Acta* **1761**, 552-559, doi:10.1016/j.bbalip.2006.04.014 (2006).
17 Balla, T. Phosphoinositides: tiny lipids with giant impact on cell regulation. *Physiol Rev* **93**, 1019-1137, doi:10.1152/physrev.00028.2012 (2013).
18 Di Paolo, G. & De Camilli, P. Phosphoinositides in cell regulation and membrane dynamics. *Nature* **443**, 651-657, doi:10.1038/nature05185 (2006).
19 Wenk, M. R. & De Camilli, P. Protein-lipid interactions and phosphoinositide metabolism in membrane traffic: insights from vesicle recycling in nerve terminals. *Proc Natl Acad Sci U S A* **101**, 8262-8269, doi:10.1073/pnas.0401874101 (2004).
20 Behnia, R. & Munro, S. Organelle identity and the signposts for membrane traffic. *Nature* **438**, 597-604, doi:10.1038/nature04397 (2005).
21 Wilson, M. S., Livermore, T. M. & Saiardi, A. Inositol pyrophosphates: between signalling and metabolism. *Biochem J* **452**, 369-379, doi:10.1042/BJ20130118 (2013).
22 Irvine, R. F. & Schell, M. J. Back in the water: the return of the inositol phosphates. *Nat Rev Mol Cell Biol* **2**, 327-338, doi:10.1038/35073015 (2001).
23 Williams, R. L. Mammalian phosphoinositide-specific phospholipase C. *Biochim Biophys Acta* **1441**, 255-267, doi:10.1016/s1388-1981(99)00150-x (1999).
24 Fukami, K., Inanobe, S., Kanemaru, K. & Nakamura, Y. Phospholipase C is a key enzyme regulating intracellular calcium and modulating the phosphoinositide balance. *Prog Lipid Res* **49**, 429-437, doi:10.1016/j.plipres.2010.06.001 (2010).
25 Kadamur, G. & Ross, E. M. Mammalian phospholipase C. *Annu Rev Physiol* **75**, 127-154, doi:10.1146/annurev-physiol-030212-183750 (2013).
26 Furuya, T., Kashuba, C., Docampo, R. & Moreno, S. N. A novel phosphatidylinositol-phospholipase C of Trypanosoma cruzi that is lipid modified and activated during trypomastigote to amastigote differentiation. *J Biol Chem* **275**, 6428-6438 (2000).
27 de Paulo Martins, V. *et al.* Acylation-dependent export of Trypanosoma cruzi phosphoinositide-specific phospholipase C to the outer surface of amastigotes. *J Biol Chem* **285**, 30906-30917, doi:10.1074/jbc.M110.142190 (2010).
28 Martins Vde, P., Galizzi, M., Salto, M. L., Docampo, R. & Moreno, S. N. Developmental expression of a Trypanosoma cruzi phosphoinositide-specific phospholipase C in amastigotes and stimulation of host phosphoinositide hydrolysis. *Infect Immun* **78**, 4206-4212, doi:10.1128/IAI.00473-10 (2010).
29 King-Keller, S., Moore, C. A., Docampo, R. & Moreno, S. N. Ca2+ Regulation of Trypanosoma brucei Phosphoinositide Phospholipase C. *Eukaryot Cell* **14**, 486-494, doi:10.1128/EC.00019-15 (2015).
30 Dominguez, D. C. Calcium signalling in bacteria. *Mol Microbiol* **54**, 291-297, doi:10.1111/j.1365-2958.2004.04276.x (2004).
31 Tuteja, N. & Mahajan, S. Calcium signaling network in plants: an overview. *Plant Signal Behav* **2**, 79-85, doi:10.4161/psb.2.2.4176 (2007).

32 Moreno, S. N. & Docampo, R. Calcium regulation in protozoan parasites. *Curr Opin Microbiol* **6**, 359-364 (2003).
33 Docampo, R. & Moreno, S. N. The role of Ca2+ in the process of cell invasion by intracellular parasites. *Parasitol Today* **12**, 61-65, doi:10.1016/0169-4758(96)80656-9 (1996).
34 Lu, H. G., Zhong, L., Chang, K. P. & Docampo, R. Intracellular Ca2+ pool content and signaling and expression of a calcium pump are linked to virulence in Leishmania mexicana amazonesis amastigotes. *J Biol Chem* **272**, 9464-9473, doi:10.1074/jbc.272.14.9464 (1997).
35 Moreno, S. N., Silva, J., Vercesi, A. E. & Docampo, R. Cytosolic-free calcium elevation in Trypanosoma cruzi is required for cell invasion. *J Exp Med* **180**, 1535-1540, doi:10.1084/jem.180.4.1535 (1994).
36 Huang, G., Bartlett, P. J., Thomas, A. P., Moreno, S. N. & Docampo, R. Acidocalcisomes of Trypanosoma brucei have an inositol 1,4,5-trisphosphate receptor that is required for growth and infectivity. *Proc Natl Acad Sci U S A* **110**, 1887-1892, doi:10.1073/pnas.1216955110 (2013).
37 Vercesi, A. E., Moreno, S. N. & Docampo, R. Ca2+/H+ exchange in acidic vacuoles of Trypanosoma brucei. *Biochem J* **304 (Pt 1)**, 227-233, doi:10.1042/bj3040227 (1994).
38 Docampo, R., Scott, D. A., Vercesi, A. E. & Moreno, S. N. Intracellular Ca2+ storage in acidocalcisomes of Trypanosoma cruzi. *Biochem J* **310 (Pt 3)**, 1005-1012, doi:10.1042/bj3101005 (1995).
39 Docampo, R. & Huang, G. Calcium signaling in trypanosomatid parasites. *Cell Calcium* **57**, 194-202, doi:10.1016/j.ceca.2014.10.015 (2015).
40 Huang, G., Vercesi, A. E. & Docampo, R. Essential regulation of cell bioenergetics in Trypanosoma brucei by the mitochondrial calcium uniporter. *Nat Commun* **4**, 2865, doi:10.1038/ncomms3865 (2013).
41 Ramakrishnan, S., Asady, B. & Docampo, R. Acidocalcisome-Mitochondrion Membrane Contact Sites in Trypanosoma brucei. *Pathogens* **7**, doi:10.3390/pathogens7020033 (2018).
42 Cestari, I. & Stuart, K. Inositol phosphate pathway controls transcription of telomeric expression sites in trypanosomes. *Proc Natl Acad Sci U S A* **112**, E2803-2812, doi:10.1073/pnas.1501206112 (2015).
43 Bulow, R. & Overath, P. Purification and characterization of the membrane-form variant surface glycoprotein hydrolase of Trypanosoma brucei. *J Biol Chem* **261**, 11918-11923 (1986).
44 Fox, J. A., Duszenko, M., Ferguson, M. A., Low, M. G. & Cross, G. A. Purification and characterization of a novel glycan-phosphatidylinositol-specific phospholipase C from Trypanosoma brucei. *J Biol Chem* **261**, 15767-15771 (1986).
45 Hereld, D., Krakow, J. L., Bangs, J. D., Hart, G. W. & Englund, P. T. A phospholipase C from Trypanosoma brucei which selectively cleaves the glycolipid on the variant surface glycoprotein. *J Biol Chem* **261**, 13813-13819 (1986).

46 McConville, M. J. & Ferguson, M. A. The structure, biosynthesis and function of glycosylated phosphatidylinositols in the parasitic protozoa and higher eukaryotes. *Biochem J* **294 (Pt 2)**, 305-324, doi:10.1042/bj2940305 (1993).
47 Chatterjee, S. & Mayor, S. The GPI-anchor and protein sorting. *Cell Mol Life Sci* **58**, 1969-1987, doi:10.1007/PL00000831 (2001).
48 Kinoshita, T. Glycosylphosphatidylinositol (GPI) Anchors: Biochemistry and Cell Biology: Introduction to a Thematic Review Series. *J Lipid Res* **57**, 4-5, doi:10.1194/jlr.E065417 (2016).
49 Pays, E. & Nolan, D. P. Expression and function of surface proteins in Trypanosoma brucei. *Mol Biochem Parasitol* **91**, 3-36, doi:10.1016/s0166-6851(97)00183-7 (1998).
50 Sunter, J., Webb, H. & Carrington, M. Determinants of GPI-PLC localisation to the flagellum and access to GPI-anchored substrates in trypanosomes. *PLoS Pathog* **9**, e1003566, doi:10.1371/journal.ppat.1003566 (2013).
51 Smith, T. K. *et al.* Blocking variant surface glycoprotein synthesis in Trypanosoma brucei triggers a general arrest in translation initiation. *PLoS One* **4**, e7532, doi:10.1371/journal.pone.0007532 (2009).
52 Pal, A., Hall, B. S., Jeffries, T. R. & Field, M. C. Rab5 and Rab11 mediate transferrin and anti-variant surface glycoprotein antibody recycling in Trypanosoma brucei. *Biochem J* **374**, 443-451, doi:10.1042/BJ20030469 (2003).
53 Mansfield, J. M. & Paulnock, D. M. Regulation of innate and acquired immunity in African trypanosomiasis. *Parasite Immunol* **27**, 361-371, doi:10.1111/j.1365-3024.2005.00791.x (2005).
54 Engstler, M. *et al.* Hydrodynamic flow-mediated protein sorting on the cell surface of trypanosomes. *Cell* **131**, 505-515, doi:10.1016/j.cell.2007.08.046 (2007).
55 Bolow, R. *et al.* Intracellular localization of the glycosyl-phosphatidylinositol-specific phospholipase C of Trypanosoma brucei. *J Cell Sci* **93 (Pt 2)**, 233-240 (1989).
56 Armah, D. A. & Mensa-Wilmot, K. S-myristoylation of a glycosylphosphatidylinositol-specific phospholipase C in Trypanosoma brucei. *J Biol Chem* **274**, 5931-5938, doi:10.1074/jbc.274.9.5931 (1999).
57 Paturiaux-Hanocq, F. *et al.* A role for the dynamic acylation of a cluster of cysteine residues in regulating the activity of the glycosylphosphatidylinositol-specific phospholipase C of Trypanosoma brucei. *J Biol Chem* **275**, 12147-12155, doi:10.1074/jbc.275.16.12147 (2000).
58 Sugiyama, G. *et al.* Phospholipase C-related but catalytically inactive protein, PRIP as a scaffolding protein for phospho-regulation. *Adv Biol Regul* **53**, 331-340, doi:10.1016/j.jbior.2013.07.001 (2013).
59 Kanematsu, T. *et al.* A new inositol 1,4,5-trisphosphate binding protein similar to phospholipase C-delta 1. *Biochem J* **313 (Pt 1)**, 319-325, doi:10.1042/bj3130319 (1996).
60 Kanematsu, T. *et al.* Putative inositol 1,4,5-trisphosphate binding proteins in rat brain cytosol. *J Biol Chem* **267**, 6518-6525 (1992).

61 Yoshida, M. *et al.* D-myo-inositol 1,4,5-trisphosphate-binding proteins in rat brain membranes. *J Biochem* **115**, 973-980, doi:10.1093/oxfordjournals.jbchem.a124447 (1994).
62 Ribeiro, A. J. M. *et al.* Emerging concepts in pseudoenzyme classification, evolution, and signaling. *Sci Signal* **12**, doi:10.1126/scisignal.aat9797 (2019).
63 Pils, B. & Schultz, J. Inactive enzyme-homologues find new function in regulatory processes. *J Mol Biol* **340**, 399-404, doi:10.1016/j.jmb.2004.04.063 (2004).
64 Todd, A. E., Orengo, C. A. & Thornton, J. M. Sequence and structural differences between enzyme and nonenzyme homologs. *Structure* **10**, 1435-1451, doi:10.1016/s0969-2126(02)00861-4 (2002).
65 Murphy, J. M., Mace, P. D. & Eyers, P. A. Live and let die: insights into pseudoenzyme mechanisms from structure. *Curr Opin Struct Biol* **47**, 95-104, doi:10.1016/j.sbi.2017.07.004 (2017).
66 Lonetti, A. *et al.* Identification of an evolutionarily conserved family of inorganic polyphosphate endopolyphosphatases. *J Biol Chem* **286**, 31966-31974, doi:10.1074/jbc.M111.266320 (2011).
67 Norbis, F. *et al.* Identification of a cDNA/protein leading to an increased Pi-uptake in Xenopus laevis oocytes. *J Membr Biol* **156**, 19-24, doi:10.1007/s002329900183 (1997).
68 Saiardi, A., Bhandari, R., Resnick, A. C., Snowman, A. M. & Snyder, S. H. Phosphorylation of proteins by inositol pyrophosphates. *Science* **306**, 2101-2105, doi:10.1126/science.1103344 (2004).
69 Jadav, R. S., Chanduri, M. V., Sengupta, S. & Bhandari, R. Inositol pyrophosphate synthesis by inositol hexakisphosphate kinase 1 is required for homologous recombination repair. *J Biol Chem* **288**, 3312-3321, doi:10.1074/jbc.M112.396556 (2013).
70 Luo, H. R. *et al.* Inositol pyrophosphates are required for DNA hyperrecombination in protein kinase c1 mutant yeast. *Biochemistry* **41**, 2509-2515, doi:10.1021/bi0118153 (2002).
71 Martin, T. F. PI(4,5)P(2) regulation of surface membrane traffic. *Curr Opin Cell Biol* **13**, 493-499, doi:10.1016/s0955-0674(00)00241-6 (2001).
72 Janetopoulos, C. & Devreotes, P. Phosphoinositide signaling plays a key role in cytokinesis. *J Cell Biol* **174**, 485-490, doi:10.1083/jcb.200603156 (2006).
73 Saiardi, A., Resnick, A. C., Snowman, A. M., Wendland, B. & Snyder, S. H. Inositol pyrophosphates regulate cell death and telomere length through phosphoinositide 3-kinase-related protein kinases. *Proc Natl Acad Sci U S A* **102**, 1911-1914, doi:10.1073/pnas.0409322102 (2005).
74 York, S. J., Armbruster, B. N., Greenwell, P., Petes, T. D. & York, J. D. Inositol diphosphate signaling regulates telomere length. *J Biol Chem* **280**, 4264-4269, doi:10.1074/jbc.M412070200 (2005).
75 Morrison, B. H., Bauer, J. A., Kalvakolanu, D. V. & Lindner, D. J. Inositol hexakisphosphate kinase 2 mediates growth suppressive and apoptotic effects of interferon-beta in ovarian carcinoma cells. *J Biol Chem* **276**, 24965-24970, doi:10.1074/jbc.M101161200 (2001).

76 Nagata, E. *et al.* Inositol hexakisphosphate kinase-2, a physiologic mediator of cell death. *J Biol Chem* **280**, 1634-1640, doi:10.1074/jbc.M409416200 (2005).
77 Szijgyarto, Z., Garedew, A., Azevedo, C. & Saiardi, A. Influence of inositol pyrophosphates on cellular energy dynamics. *Science* **334**, 802-805, doi:10.1126/science.1211908 (2011).
78 Illies, C. *et al.* Requirement of inositol pyrophosphates for full exocytotic capacity in pancreatic beta cells. *Science* **318**, 1299-1302, doi:10.1126/science.1146824 (2007).
79 Burton, A., Azevedo, C., Andreassi, C., Riccio, A. & Saiardi, A. Inositol pyrophosphates regulate JMJD2C-dependent histone demethylation. *Proc Natl Acad Sci U S A* **110**, 18970-18975, doi:10.1073/pnas.1309699110 (2013).
80 Yin, H. L. & Janmey, P. A. Phosphoinositide regulation of the actin cytoskeleton. *Annu Rev Physiol* **65**, 761-789, doi:10.1146/annurev.physiol.65.092101.142517 (2003).
81 Sechi, A. S. & Wehland, J. The actin cytoskeleton and plasma membrane connection: PtdIns(4,5)P(2) influences cytoskeletal protein activity at the plasma membrane. *J Cell Sci* **113 Pt 21**, 3685-3695 (2000).
82 Nagata, E. *et al.* Inositol hexakisphosphate kinases promote autophagy. *Int J Biochem Cell Biol* **42**, 2065-2071, doi:10.1016/j.biocel.2010.09.013 (2010).
83 Potapenko, E. *et al.* 5-Diphosphoinositol pentakisphosphate (5-IP7) regulates phosphate release from acidocalcisomes and yeast vacuoles. *J Biol Chem* **293**, 19101-19112, doi:10.1074/jbc.RA118.005884 (2018).
84 Cestari, I., Anupama, A. & Stuart, K. Inositol polyphosphate multikinase regulation of Trypanosoma brucei life stage development. *Mol Biol Cell* **29**, 1137-1152, doi:10.1091/mbc.E17-08-0515 (2018).
85 Stephens, L. *et al.* The detection, purification, structural characterization, and metabolism of diphosphoinositol pentakisphosphate(s) and bisdiphosphoinositol tetrakisphosphate(s). *J Biol Chem* **268**, 4009-4015 (1993).
86 Stephens, L. R. & Irvine, R. F. Stepwise phosphorylation of myo-inositol leading to myo-inositol hexakisphosphate in Dictyostelium. *Nature* **346**, 580-583, doi:10.1038/346580a0 (1990).
87 Brearley, C. A. & Hanke, D. E. Metabolic evidence for the order of addition of individual phosphate esters in the myo-inositol moiety of inositol hexakisphosphate in the duckweed Spirodela polyrhiza L. *Biochem J* **314 (Pt 1)**, 227-233, doi:10.1042/bj3140227 (1996).
88 Aslett, M. *et al.* TriTrypDB: a functional genomic resource for the Trypanosomatidae. *Nucleic Acids Res* **38**, D457-462, doi:10.1093/nar/gkp851 (2010).
89 Maurer-Stroh, S., Eisenhaber, B. & Eisenhaber, F. N-terminal N-myristoylation of proteins: prediction of substrate proteins from amino acid sequence. *J Mol Biol* **317**, 541-557, doi:10.1006/jmbi.2002.5426 (2002).
90 Bologna, G., Yvon, C., Duvaud, S. & Veuthey, A. L. N-Terminal myristoylation predictions by ensembles of neural networks. *Proteomics* **4**, 1626-1632, doi:10.1002/pmic.200300783 (2004).

91 Mitchell, A. L. *et al.* InterPro in 2019: improving coverage, classification and access to protein sequence annotations. *Nucleic Acids Res* **47**, D351-D360, doi:10.1093/nar/gky1100 (2019).
92 Sievers, F. & Higgins, D. G. Clustal Omega for making accurate alignments of many protein sequences. *Protein Sci* **27**, 135-145, doi:10.1002/pro.3290 (2018).
93 Zhang, Y. I-TASSER server for protein 3D structure prediction. *BMC Bioinformatics* **9**, 40, doi:10.1186/1471-2105-9-40 (2008).
94 Roy, A., Kucukural, A. & Zhang, Y. I-TASSER: a unified platform for automated protein structure and function prediction. *Nat Protoc* **5**, 725-738, doi:10.1038/nprot.2010.5 (2010).
95 Yang, J. *et al.* The I-TASSER Suite: protein structure and function prediction. *Nat Methods* **12**, 7-8, doi:10.1038/nmeth.3213 (2015).
96 Fischer, S. *et al.* Using OrthoMCL to assign proteins to OrthoMCL-DB groups or to cluster proteomes into new ortholog groups. *Curr Protoc Bioinformatics* **Chapter 6**, Unit 6 12 11-19, doi:10.1002/0471250953.bi0612s35 (2011).
97 Katoh, K. & Standley, D. M. MAFFT multiple sequence alignment software version 7: improvements in performance and usability. *Mol Biol Evol* **30**, 772-780, doi:10.1093/molbev/mst010 (2013).
98 Posada, D. & Crandall, K. A. MODELTEST: testing the model of DNA substitution. *Bioinformatics* **14**, 817-818, doi:10.1093/bioinformatics/14.9.817 (1998).
99 Guindon, S. *et al.* New algorithms and methods to estimate maximum-likelihood phylogenies: assessing the performance of PhyML 3.0. *Syst Biol* **59**, 307-321, doi:10.1093/sysbio/syq010 (2010).
100 Ding, Z. *et al.* Binding of inositol 1,4,5-trisphosphate (IP3) and adenophostin A to the N-terminal region of the IP3 receptor: thermodynamic analysis using fluorescence polarization with a novel IP3 receptor ligand. *Mol Pharmacol* **77**, 995-1004, doi:10.1124/mol.109.062596 (2010).
101 Huang, G. *et al.* Adaptor protein-3 (AP-3) complex mediates the biogenesis of acidocalcisomes and is essential for growth and virulence of Trypanosoma brucei. *J Biol Chem* **286**, 36619-36630, doi:10.1074/jbc.M111.284661 (2011).
102 Cunningham, I. New culture medium for maintenance of tsetse tissues and growth of trypanosomatids. *J Protozool* **24**, 325-329, doi:10.1111/j.1550-7408.1977.tb00987.x (1977).
103 Wirtz, E., Leal, S., Ochatt, C. & Cross, G. A. A tightly regulated inducible expression system for conditional gene knock-outs and dominant-negative genetics in Trypanosoma brucei. *Mol Biochem Parasitol* **99**, 89-101, doi:10.1016/s0166-6851(99)00002-x (1999).
104 Hirumi, H. & Hirumi, K. Continuous cultivation of Trypanosoma brucei blood stream forms in a medium containing a low concentration of serum protein without feeder cell layers. *J Parasitol* **75**, 985-989 (1989).
105 Redmond, S., Vadivelu, J. & Field, M. C. RNAit: an automated web-based tool for the selection of RNAi targets in Trypanosoma brucei. *Mol Biochem Parasitol* **128**, 115-118, doi:10.1016/s0166-6851(03)00045-8 (2003).

106 LaCount, D. J., Barrett, B. & Donelson, J. E. Trypanosoma brucei FLA1 is required for flagellum attachment and cytokinesis. *J Biol Chem* **277**, 17580-17588, doi:10.1074/jbc.M200873200 (2002).
107 Oberholzer, M., Morand, S., Kunz, S. & Seebeck, T. A vector series for rapid PCR-mediated C-terminal in situ tagging of Trypanosoma brucei genes. *Mol Biochem Parasitol* **145**, 117-120, doi:10.1016/j.molbiopara.2005.09.002 (2006).
108 Couso, I. *et al.* Synergism between Inositol Polyphosphates and TOR Kinase Signaling in Nutrient Sensing, Growth Control, and Lipid Metabolism in Chlamydomonas. *Plant Cell* **28**, 2026-2042, doi:10.1105/tpc.16.00351 (2016).
109 Wylie, K. M., Schrimpf, J. E. & Morrison, L. A. Increased eIF2alpha phosphorylation attenuates replication of herpes simplex virus 2 vhs mutants in mouse embryonic fibroblasts and correlates with reduced accumulation of the PKR antagonist ICP34.5. *J Virol* **83**, 9151-9162, doi:10.1128/JVI.00886-09 (2009).
110 Gietz, R. D. & Schiestl, R. H. High-efficiency yeast transformation using the LiAc/SS carrier DNA/PEG method. *Nat Protoc* **2**, 31-34, doi:10.1038/nprot.2007.13 (2007).
111 Lemercier, G. *et al.* A vacuolar-type H+-pyrophosphatase governs maintenance of functional acidocalcisomes and growth of the insect and mammalian forms of Trypanosoma brucei. *J Biol Chem* **277**, 37369-37376, doi:10.1074/jbc.M204744200 (2002).
112 Herbert, W. J. & Lumsden, W. H. Trypanosoma brucei: a rapid "matching" method for estimating the host's parasitemia. *Exp Parasitol* **40**, 427-431, doi:10.1016/0014-4894(76)90110-7 (1976).
113 Emmer, B. T. *et al.* Global analysis of protein palmitoylation in African trypanosomes. *Eukaryot Cell* **10**, 455-463, doi:10.1128/EC.00248-10 (2011).
114 Flegontov, P. *et al.* Paratrypanosoma is a novel early-branching trypanosomatid. *Curr Biol* **23**, 1787-1793, doi:10.1016/j.cub.2013.07.045 (2013).
115 Willert, E. K., Fitzpatrick, R. & Phillips, M. A. Allosteric regulation of an essential trypanosome polyamine biosynthetic enzyme by a catalytically dead homolog. *Proc Natl Acad Sci U S A* **104**, 8275-8280, doi:10.1073/pnas.0701111104 (2007).
116 Nguyen, S., Jones, D. C., Wyllie, S., Fairlamb, A. H. & Phillips, M. A. Allosteric activation of trypanosomatid deoxyhypusine synthase by a catalytically dead paralog. *J Biol Chem* **288**, 15256-15267, doi:10.1074/jbc.M113.461137 (2013).
117 Kafkova, L. *et al.* The Major Protein Arginine Methyltransferase in Trypanosoma brucei Functions as an Enzyme-Prozyme Complex. *J Biol Chem* **292**, 2089-2100, doi:10.1074/jbc.M116.757112 (2017).
118 Vertommen, D. *et al.* Differential expression of glycosomal and mitochondrial proteins in the two major life-cycle stages of Trypanosoma brucei. *Mol Biochem Parasitol* **158**, 189-201, doi:10.1016/j.molbiopara.2007.12.008 (2008).
119 Ivarsson, Y. Plasticity of PDZ domains in ligand recognition and signaling. *FEBS Lett* **586**, 2638-2647, doi:10.1016/j.febslet.2012.04.015 (2012).
120 Wawrzyniak, A. M., Kashyap, R. & Zimmermann, P. Phosphoinositides and PDZ domain scaffolds. *Adv Exp Med Biol* **991**, 41-57, doi:10.1007/978-94-007-6331-9_4 (2013).

121 Zimmermann, P. *et al.* PIP(2)-PDZ domain binding controls the association of syntenin with the plasma membrane. *Mol Cell* **9**, 1215-1225 (2002).
122 Mortier, E. *et al.* Nuclear speckles and nucleoli targeting by PIP2-PDZ domain interactions. *EMBO J* **24**, 2556-2565, doi:10.1038/sj.emboj.7600722 (2005).
123 Krojer, T., Garrido-Franco, M., Huber, R., Ehrmann, M. & Clausen, T. Crystal structure of DegP (HtrA) reveals a new protease-chaperone machine. *Nature* **416**, 455-459, doi:10.1038/416455a (2002).
124 Subota, I. *et al.* Proteomic analysis of intact flagella of procyclic Trypanosoma brucei cells identifies novel flagellar proteins with unique sub-localization and dynamics. *Mol Cell Proteomics* **13**, 1769-1786, doi:10.1074/mcp.M113.033357 (2014).
125 Yang, M., Jensen, R. E., Yaffe, M. P., Oppliger, W. & Schatz, G. Import of proteins into yeast mitochondria: the purified matrix processing protease contains two subunits which are encoded by the nuclear MAS1 and MAS2 genes. *EMBO J* **7**, 3857-3862 (1988).
126 Kramer, S. *et al.* The RNA helicase DHH1 is central to the correct expression of many developmentally regulated mRNAs in trypanosomes. *J Cell Sci* **123**, 699-711, doi:10.1242/jcs.058511 (2010).
127 Pitula, J. S., Park, J., Parsons, M., Ruyechan, W. T. & Williams, N. Two families of RNA binding proteins from Trypanosoma brucei associate in a direct protein-protein interaction. *Mol Biochem Parasitol* **122**, 81-89, doi:10.1016/s0166-6851(02)00076-2 (2002).
128 Pitula, J., Ruyechan, W. T. & Williams, N. Two novel RNA binding proteins from Trypanosoma brucei are associated with 5S rRNA. *Biochem Biophys Res Commun* **290**, 569-576, doi:10.1006/bbrc.2001.6226 (2002).
129 Dreyfuss, G., Swanson, M. S. & Pinol-Roma, S. Heterogeneous nuclear ribonucleoprotein particles and the pathway of mRNA formation. *Trends Biochem Sci* **13**, 86-91, doi:10.1016/0968-0004(88)90046-1 (1988).
130 Chambers, J. C., Kenan, D., Martin, B. J. & Keene, J. D. Genomic structure and amino acid sequence domains of the human La autoantigen. *J Biol Chem* **263**, 18043-18051 (1988).
131 Sachs, A. B., Davis, R. W. & Kornberg, R. D. A single domain of yeast poly(A)-binding protein is necessary and sufficient for RNA binding and cell viability. *Mol Cell Biol* **7**, 3268-3276, doi:10.1128/mcb.7.9.3268 (1987).
132 Query, C. C., Bentley, R. C. & Keene, J. D. A common RNA recognition motif identified within a defined U1 RNA binding domain of the 70K U1 snRNP protein. *Cell* **57**, 89-101, doi:10.1016/0092-8674(89)90175-x (1989).
133 Widjaja, M. *et al.* Elongation factor Tu is a multifunctional and processed moonlighting protein. *Sci Rep* **7**, 11227, doi:10.1038/s41598-017-10644-z (2017).
134 Bringaud, F. *et al.* A new, expressed multigene family containing a hot spot for insertion of retroelements is associated with polymorphic subtelomeric regions of Trypanosoma brucei. *Eukaryot Cell* **1**, 137-151, doi:10.1128/ec.1.1.137-151.2002 (2002).
135 Oberholzer, M. *et al.* Independent analysis of the flagellum surface and matrix proteomes provides insight into flagellum signaling in mammalian-infectious

Trypanosoma brucei. *Mol Cell Proteomics* **10**, M111 010538, doi:10.1074/mcp.M111.010538 (2011).
136 Rios, E. The cell boundary theorem: a simple law of the control of cytosolic calcium concentration. *J Physiol Sci* **60**, 81-84, doi:10.1007/s12576-009-0069-z (2010).
137 Nolan, D. P., Reverlard, P. & Pays, E. Overexpression and characterization of a gene for a Ca(2+)-ATPase of the endoplasmic reticulum in Trypanosoma brucei. *J Biol Chem* **269**, 26045-26051 (1994).
138 Huang, G. & Docampo, R. The Mitochondrial Ca(2+) Uniporter Complex (MCUC) of Trypanosoma brucei Is a Hetero-oligomer That Contains Novel Subunits Essential for Ca(2+) Uptake. *MBio* **9**, doi:10.1128/mBio.01700-18 (2018).
139 Docampo, R., de Souza, W., Miranda, K., Rohloff, P. & Moreno, S. N. Acidocalcisomes - conserved from bacteria to man. *Nat Rev Microbiol* **3**, 251-261, doi:10.1038/nrmicro1097 (2005).
140 Beck, M. *et al.* The quantitative proteome of a human cell line. *Mol Syst Biol* **7**, 549, doi:10.1038/msb.2011.82 (2011).